CZECH TECHNICAL UNIVERSITY IN PRAGUE

Faculty of Nuclear Sciences and Physical Engineering

Department of Physics

Diploma thesis

Study of Nuclear Effects in Proton (Deuteron) – Nuclear Collisions at RHIC and LHC Energies

Jan Čepila

Supervisor: RNDr. Ján Nemčík CSc.

Prague, 2008

ČESKÉ VYSOKÉ UČENÍ TECHNICKÉ
V PRAZE
Fakulta Jaderná a Fyzikálně Inženýrská
Katedra Fyziky

Diplomová práce

Studium jaderných efektů v proton (deuteron) – jaderných srážkách při energiích RHIC a LHC

Jan Čepila

Supervisor: RNDr. Ján Nemčík CSc.

Praha, 2008

ČESKÉ VYSOKÉ UČENÍ TECHNICKÉ V PRAZE
FAKULTA JADERNÁ A FYZIKÁLNĚ INŽENÝRSKÁ
PRAHA 1 - STARÉ MĚSTO, BŘEHOVÁ 7 - PSČ 115 19

Katedra: fyziky *Akademický rok:* 2007/08

ZADÁNÍ DIPLOMOVÉ PRÁCE

Posluchač: Jan Čepila

Obor: Jaderné inženýrství

Zaměření: Experimentální jaderná fyzika

Název práce: Studium jaderných efektů v proton (deuteron) – jaderných srážkách při energiích RHIC a LHC

Název práce: (anglicky) Study of Nuclear Effects in Proton (Deuteron) – Nuclear Collisions at RHIC and LHC Energies

Osnova:

Studium jaderných efektů v hadron-jaderných interakcích a v srážkách těžkých iontů představuje v současnosti hlavní těžiště fyzikálního výzkumu jednak v experimentální oblasti hlavně na urychlovači RHIC jako i v teoretické oblasti při interpretaci dosažených experimentálních výsledků. Tato diplomová práce má proto přispět k fenomenologickému popisu a fyzikálnímu chápání jaderných efektů některých procesů (produkce Drell-Yanovských párů, produkce přímých fotonů), které budou experimentálně měřeny v roce 2008 v připravovaných interakcích deuteronového svazku s Au terčíkem na urychlovači RHIC. Kromě toho daný fenomenologický přístup založený na přiblížení barevného dipólu umožní dát relevantní předpovědi očekávaných jaderných efektů i při vyšších energiích, odpovídajících připravovaným experimentům na urychlovači LHC v CERN.

Doporučená literatura:

1. Cheuk-Yin Wong, Introduction to High-Energy Heavy-Ion Collisions, Singapore, Singapore: World Scientific (1994).

2. J. Raufeisen, QCD Coherence Effects in High-Energy Reactions with Nuclei, Ph.D. Thesis, 2000, e-Print: hep-ph/0009358.

3. B.Z. Kopeliovich, J. Raufeisen and A.V. Tarasov, Phys. Lett. B503, 91 (2001), e-Print: hep-ph/0012035.

4. B.Z. Kopeliovich, J. Raufeisen and A.V. Tarasov, Phys. Rev. C67, 014903 (2003), e-Print: hep-ph/0110221.

Jméno a pracoviště vedoucího diplomové práce:

RNDr. Ján Nemčík, CSc., KF FJFI ČVUT

Do diplomové práce se vkládá zadání a dále na stranu předcházející obsahu abstrakt a klíčová slova. Součástí zadání diplomové práce je její uložení na webové stránky katedry fyziky ve formátu LaTex a zaslání abstraktu a klíčových slov ve formátu WORD na e-mailovou adresu katedry fyziky: kf@fjfi.cvut.cz

Datum zadání diplomové práce: 30.10.2007

Termín odevzdání diplomové práce: 09.05.2008

....

Vedoucí katedry *Děkan*

ČESKÉ VYSOKÉ UČENÍ TECHNICKÉ V PRAZE Fakulta jaderná a fyzikálně inženýrská -1-

V Praze dne 30.10.2007

Prohlášení:

Prohlašuji, že jsem svou diplomovou práci vypracoval samostatně a použil jsem pouze podklady (literaturu, software, atd.) uvedené v přiloženém seznamu.

Nemám závažný důvod proti užití tohoto školního díla ve smyslu 60 Zákona č.121/2000 Sb., o právu autorském, o právech souvisejících s právem autorským a o změně některých zákonů (autorský zákon).

V Praze dne

Title:
Study of Nuclear Effects in Proton (Deuteron) – Nuclear Collisions at RHIC and LHC Energies

Author: Jan Čepila

Specialization: Experimental nuclear physics

Sort of project: Diploma thesis

Supervisor: RNDr. Ján Nemčík, CSc. Department of Physics, Faculty of Nuclear Physics and Physical Engineering, Czech Technical University in Prague. Institute of Experimental Physics SAS, Košice

Consultant:

Abstract: The currently most widespread theory for the description of hadron - hadron and hadron - nucleus collisions is a parton model. However, some apparent failings of this model (mainly in hadron - nucleus collisions) lead to the formulation of other approaches to the description of a collision and to the calculation of cross sections. The color dipole approach can be successively used in the region of deep inelastic scattering for the formulation of a theory which describes appropriate collisions better than existing parton model. The same approach can be used to the description of the direct photon production and the Drell-Yan lepton pair production also, for what this work is dedicated to. A summary of theoretical calculations is presented here for the understanding of the whole model. The main feature this thesis is devoted to is a nuclear modification factor for proton - nucleus and deuteron - nucleus collisions and a prediction for RHIC energies with further outlook to LHC energies. This factor can be used to the estimate of the size of nuclear effects in contrast to hadron - hadron collisions - mainly nuclear shadowing and Cronin effect.

Key words: Drell-Yan process, direct photon production, color dipole approach, nuclear modification factor, nuclear shadowing, RHIC.

Název práce:
Studium jaderných efektů v proton (deuteron) – jaderných srážkách při energiích RHIC a LHC

Autor: Jan Čepila

Abstrakt: Partonový model je v současnosti nejrozšířenější teorií používanou pro popis hadron - hadronových a hadron - jaderných srážek. Některé zjevné nedostatky tohoto modelu (především v hadron - jaderných srážkách) ovšem vedou k formulaci jiných přístupů k popisu srážky a výpočtu účinných průřezů. V oblasti hluboce nepružného rozptylu lze s úspěchem použít přiblížení barevného dipólu pro formulaci teorie, která popisuje zmíněné srážky lépe než stávající partonový model. Zmíněný postup se ovšem dá použít i na analýzu mechanismu produkce přímých fotonů a Drell-Yanových leptonových párů, čemuž je věnována tato práce. Je zde prezentován souhrn teoretických výpočtů pro pochopení celého modelu. Konkrétní vlastnost, které je věnována tato práce je jaderný modifikační faktor pro proton - jaderné a deuteron - jaderné srážky a jeho předpověď pro energie odpovídající urychlovači RHIC s výhledem na pokračování k energiím na urychlovači LHC. Pomocí něho lze usoudit na míru jaderných efektů oproti hadron - hadronovým srážkám - především jaderného stínění a Croninova efektu.

Klíčová slova: Drell-Yanův proces, produkce přímých fotonů, přiblížení barevného dipólu, jaderný modifikační faktor, jaderné stínění, RHIC.

Acknowledgement

First of all, I would like to thank to Dr. Ján Nemčík from FNSPE CTU & ÚEF SAV Košice for his invaluable help, motivation and guidance throughout the preparation of this work. Also I appreciate his time spent on reading through my work and language and factual corrections. I am grateful to doc.RNDr. Vojtěch Petráček, CSc. for his support during my studies at the Department of Physics of FNSPE.

I also express my gratitude to those, who gave me occasional, but very helpful, pieces of advice in different topics, mainly from the team of the Experimental physics at the Department of Physics on FNSPE.

Contents

List of Figures

List of Abbreviations

A-A	nucleus-nucleus
d-A	deuteron-nucleus
DGLAP	Dokshitzer-Gribov-Lipatov-Altarelli-Parisi
DIS	Deep Inelastic Scattering
DP	Direct Photon
DY	The Drell-Yan
EMC	The European Muon Collaboration
GVDM	generalized vector dominance model
LC	Light-cone
LO	Leading Order
LPM	Landau-Pomeranchuk-Migdal
NLO	Next-to-leading order
NNLO	Next-to-next-to-leading order
p-A	proton-nucleus
p-p	proton-proton
PDF	Proton Distribution Function
pQCD	perturbative Quantum Chromodynamics
PT	Perturbative theory
QCD	Quantum Chromodynamics
VDM	vector dominance model

Chapter 1

Introduction

This project is devoted to the study of nuclear effects in proton - nucleus and deuteron - nucleus collisions mainly on RHIC energies and further to the LHC. The use of nuclei in high-energy collisions have certain advantages in contrast to proton collisions. In principle, we can study scattering products from proton collisions with a detector located within a macroscopic distance from the collision point in contrast to a nuclear medium, which can serve as detector itself. Therefore we can study coherence effects in QCD not accessible in proton collisions. The transition from the description of a proton - proton collision to the description of a proton - nucleus (nucleus - nucleus) collision is not as straightforward as it seems. Naively, it could be expected that the cross section for proton - nucleus collisions is equal to A times the cross section for proton - proton collisions. But as experiments suggest, there are some collective effects that disrupt this idea. When one tries to calculate the cross section in proton - nucleus collisions with the factorization theorem and PDF´s from the deep inelastic scattering, it is almost impossible to reconstruct some well known experimental features as nuclear broadening of p_T spectra. Also the calculated nuclear shadowing appears to be independent of centrality, which is in contrast with experimental facts.
There exists a model for the deep inelastic scattering(DIS) based on color dipole approach[9]. In the DIS, a lepton is scattered off a proton. This lepton radiates a virtual photon, which probes a structure of the proton and therefore it can give a clue to the constitution of a proton. The process suggests the existence of three so called valence quarks. These quarks carry together quantum numbers of a proton. Other than valence quarks, there seems to be particles from "quantum sea". Mainly it consists of gluons, that mediate the color force between quarks. Since gluons do not have an electric charge, they cannot be visible with the DIS. But quarks seem to carry only a half of momentum of proton and therefore there have to be some sort of neutral particles - sea particles. The energy of collisions has to be raised in order to resolve the structure in more details. As a consequence, instead of seeing a quark with a longitudinal momentum fraction Bjorken x we see a quark with a gluon carrying together the

same Bjorken x and so each carrying lesser part. For sufficiently high energies, most of momentum can be carried by gluons. Furthermore, gluons can split to quark - antiquark pairs and increase quark density. For extremely high energies - $x_{Bj} << 0.1$ - the partonic content of proton is dominated by gluons and a scattered photon sees only sea quarks. This process, however, do not distinguish between quark and antiquark density so we have to study the Drell-Yan process as a complementary one.
The explanation of the DIS off nuclei depends on the reference frame. In the infinite momentum frame, nucleus is Lorentz contracted and the localization of gluons is given by uncertainty relations. Therefore, the gluon cloud is spread over the whole nucleus and nucleons can "communicate" with each other. In the rest frame of a nucleus distances between nucleons are much bigger and so they can be considered as independent particles. As the cross section is Lorentz invariant, the partonic interpretation of the process has to be frame dependent. The result is that both parton distribution in nucleus and interpretation what partons are has to be frame dependent.
The DIS in the rest frame of a nucleus can be described as a process, where a lepton radiates virtual photon, that fluctuates to a quark - antiquark pair (as color dipole)[3].

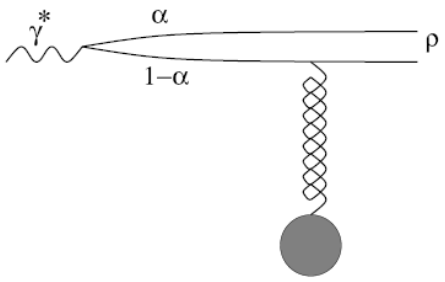

Figure 1.1: A deep inelastic scattering scheme using color dipole idea

This coherent fluctuation is then disrupted by color interaction with different nucleons. That corresponds to the overlap of gluon clouds in the infinite momentum frame. A long timelife of the fluctuation leads to the existence of coherence effects observed in experiment.
The same approach can be applied to the Drell-Yan process. In the nucleus rest frame it looks like a bremsstrahlung of a photon, which decays to a lepton pair. Moreover, the cross section can be expressed using the **same** dipole cross section from the DIS[2].

That is a direct consequence of a factorization theorem. When a quark passes through the nucleus, it undergoes several scattering from nucleons. The effect of multiple scattering of quark on its bremsstrahlung is known from QED as Landau-Pomeranchuk-Migdal effect[15] [16], that leads to a reduction of the cross section due to destructive interferences. This effect can be seen on a

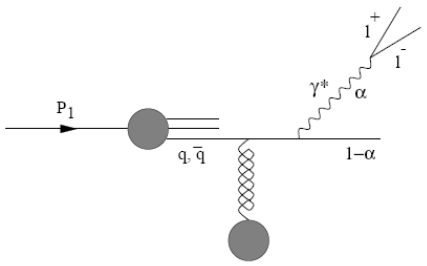

Figure 1.2: A Drell-Yan production scheme in a target rest frame

nuclear modification factor, which is presented here. Even stronger effect can be seen for direct photon production, which differs from the Drell-Yan process only in the fact that emitted photon is real and do not decay into lepton pair. Next chapter consists of the description of the Dell-Yan process in classical parton model. The third chapter than repeats the calculation in a color dipole approach. Fourth chapter is devoted to the discussion about a parametrization used for describing the dipole cross section and various PDF‘s used for the calculation. In the fifth chapter various nuclear effects expected in nuclear collisions are discussed. The last chapter summarizes results of calculations performed in this model and the prediction of nuclear modification factors for RHIC accelerator.

Chapter 2

The Drell-Yan process in a parton model

2.1 QCD factorization theorem for Drell-Yan process

At high energy hadron colliders, we can distinguish two types of scattering processes. Higgs boson and high p_T jet production are denoted as hard processes and their rates and properties can be predicted very well with perturbation theory. The total cross-section and underlying events are called soft processes, which are lead by non-perturbative QCD effects. All those processes are still described by the QCD theory. Furthermore, hard processes are followed by soft interactions and therefore they have to be well analyzed to obtain comparable predictions from perturbative approach. The factorization in QCD can be used to obtain such hard scattering cross-sections in hadron-hadron collisions. Here we will restrict to leading order processes (LO). The factorization theorem comes from Drell and Yan[11]. They suggested that the parton model ideas which comes from the deep inelastic scattering can be used on certain processes in hadron-hadron collisions. They studied the production of massive lepton pair by quark-antiquark annihilation. They postulated that the hadronic cross-section of the process $AB \to e^+e^- + X$ is[11]

$$\sigma_{AB} = \int \mathrm{d}x_a \mathrm{d}x_b f_{a/A}(x_a) f_{b/B}(x_b) \hat{\sigma}_{q\bar{q}\to e^+e^-} \tag{2.1}$$

where $f_{g/A}(x)$ are parton distribution functions from the deep inelastic scattering. The domain of validity is the asymptotic limit (in analogy of Bjorken scaling limit) $\tau = \frac{M^2_{l^+l^-}}{s}|_{s\to+\infty}$ fixed. The same approach can be used to other hard scattering processes. Problems arise when we calculate perturbative corrections from real and virtual gluon emission. Large logarithms from gluons emitted collinear with incoming quarks appeared to spoil the convergence of

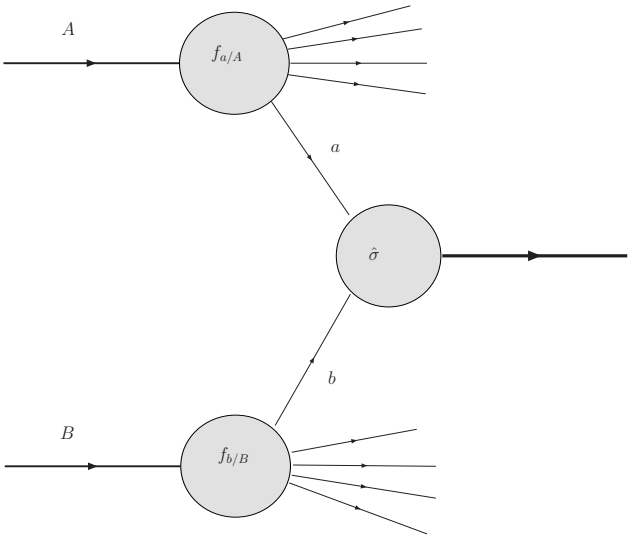

Figure 2.1: Schematics of Drell-Yan factorization theorem

the perturbative expansion. This is the same problem as in deep inelastic scattering structure function calculations. So they can be absorbed (using DGLAP equations in the definition of the parton distributions) giving rise to logarithmic violations of scaling. All logarithms from Drell-Yan corrections can be factored into renormalized parton distributions as they appear in the factorization theorem. Restricting to LO logarithm corrections we can write[6]

$$\sigma_{AB} = \int \mathrm{d}x_a \mathrm{d}x_b f_{a/A}(x_a, Q^2) f_{b/B}(x_b, Q^2) \hat{\sigma}_{q\bar{q}\to e^+e^-} \tag{2.2}$$

The factor Q^2 is a large momentum scale, which characterizes the hard scattering. Changes to the Q^2 scale of $O(1)$ are equivalent in this leading logarithm approximation. The last step is the fact that the finite corrections after factorization of logarithms had to be calculated separately for each process (perturbative $O(\alpha_S^n)$ correction to the total cross-section). Therefore

$$\sigma_{AB} = \int \mathrm{d}x_a \mathrm{d}x_b f_{a/A}(x_a, \mu_F^2) f_{b/B}(x_b, \mu_F^2) \times [\hat{\sigma}_0 + \alpha_S(\mu_R^2)\hat{\sigma}_1 + \ldots]_{q\bar{q}\to e^+e^-} \tag{2.3}$$

where μ_F is a factorization scale, which "separates" the long and short-distance physics. The μ_R is a renormalization scale for the QCD running coupling. Formally, the total cross-section (to all orders of PT) is invariant under changes in these parameters. In the absence of a complete set of higher order corrections, it is necessary to make a choice for these scales to make cross-section

predictions. For Drell-Yan process, the standard choice is $\mu_F = \mu_R = M_{l^+l^-}$. The DGLAP equations are[6]

$$\frac{\partial q_i(x,\mu^2)}{\partial \ln \mu^2} = \frac{\alpha_S}{2\pi}\int_x^1 \frac{dz}{z}[P_{q_i q_j}(z,\alpha_S)q_j(\frac{x}{z},\mu^2) + P_{q_i g}(z,\alpha_S)g(\frac{x}{z},\mu^2)] \quad (2.4)$$
$$\frac{\partial g(x,\mu^2)}{\partial \ln \mu^2} = \frac{\alpha_S}{2\pi}\int_x^1 \frac{dz}{z}[P_{g q_j}(z,\alpha_S)q_j(\frac{x}{z},\mu^2) + P_{gg}(z,\alpha_S)g(\frac{x}{z},\mu^2)]$$

where P_{ab} are splitting functions with perturbative expansion

$$P_{ab}(x,\alpha_S) = P_{ab}^{(0)}(x) + \frac{\alpha_S}{2\pi}P_{ab}^{(1)}(x) + \dots \quad (2.5)$$

.

These equations determine the Q^2 dependence of the PDF's. The x-dependence has to be obtained from fitting hard scattering data.

2.2 The parton model cross-section calculation

The Drell-Yan process, as stated before, lie in a production of vector bosons or photons in hadron - hadron interactions. Let the restriction to a photon production be valid for the purpose of our analysis considering the energy scale. Then at the partonic level, when two hadrons collide, a quark from one hadron and an antiquark from the second hadron annihilate by forming a time-like photon, which then decays to a lepton pair.

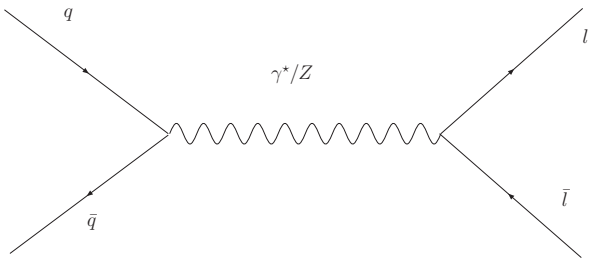

Figure 2.2: The Feynmann diagram of the Drell-Yan process

Let‘s denote a mass of a time-like photon as

$$M^2 = q^2 > 0, \quad (2.6)$$

where q^μ is a four-momentum of virtual photon.
A square of the *cms* energy is denoted as

$$s = (p_1 + p_2)^2, \quad (2.7)$$

where $p^{\mu}_{1,2}$ is a four-momentum of appropriate hadron.
At last, let's introduce a Feynmann variable as

$$x_F = \frac{2p_L^{cms}}{\sqrt{s}} \doteq x_1 - x_2, \tag{2.8}$$

where p_L^{cms} is a longitudinal momentum of a dilepton in hadron - hadron center of mass frame and $x_1 = \frac{2p_2 q}{s}, x_2 = \frac{2p_1 q}{s}$ are Bjorken variables of appropriate hadron. These variables has a meaning of a fraction of proton longitudinal momentum, which does take part in hard process. Therefore, a quark and an antiquark involved in this process have momentum $x_1 P_1$ and $x_2 P_2$ respectively. In addition, the following equation hold (neglecting p_T)

$$x_1 x_2 = \frac{M^2}{s} =: \tau \tag{2.9}$$

Structure functions for the Drell-Yan process can be extracted from a hadronic tensor[3]

$$W^{\mu\nu} = \int d^4x e^{iqx} < p_1 p_2 | J^{\mu}_{(x)} J^{\nu}_{(0)} | p_1 p_2 >, \tag{2.10}$$

which leads to four independent structure functions for Drell-Yan process (soft component). Partonic cross section (hard component) can be derived using standard Feynmann rules as

$$\frac{d\hat{\sigma}}{dM^2} = \frac{4\pi\alpha_{em}^2 Z_f^2}{3N_C M^2}\delta(x_1 x_2 s - M^2) \tag{2.11}$$

Hadronic cross section can be then written using factorization theorem as[6]

$$\frac{d\sigma}{dM^2} = \int_0^1 dx_1 dx_2 \sum_f \{q_f(x_1)\bar{q}_f(x_2) + q_f(x_2)\bar{q}_f(x_1)\}\frac{d\hat{\sigma}}{dM^2} \tag{2.12}$$

Integration over x_2 leads to a form

$$M^2\frac{d\sigma}{d\tau} = \frac{4\pi\alpha_{em}^2}{3N_C}\int_0^1 dx_1 \sum_f Z_f^2\{q_f(x_1)\bar{q}_f(\frac{\tau}{x_1}) + q_f(\frac{\tau}{x_1})\bar{q}_f(x_1)\} \tag{2.13}$$

Therefore, the final cross section depends on a scaling variable τ as confirmed by experiment.
There are, however, some features that cannot be explained by LO calculation.

- This cross section is approximately 2-3 times lesser than observed. That is why the so called K-factor is introduced to extend the cross section to a NLO value.

- In experiment, there are photons with high p_T, but it was neglected in this approach. The primordial momentum distribution of quarks can be included as a gauss distribution to correct this, but the width needed to fit the experiment is much bigger than the one that correspond with the Fermi motion.

These problems apparently vanish when we pass over to the NLO calculation. Feynmann diagrams of higher order, however, contain divergencies. Infrared divergencies vanish when we sum over all real and virtual contributions. Collinear (Bjorken) divergencies, corresponding to the situation when intermediate quark in a QCD Compton process has a $p_T \to 0$ can be absorbed to parton densities and therefore redefine parton distribution functions

$$q_f(x) \to q_f(x) + \frac{\alpha_s}{2\pi} ln(\frac{M^2}{\kappa^2}) \int_x^1 \frac{dy}{y} P_{fG}(\frac{x}{y}) G_{(y)} \tag{2.14}$$

This shows what is meant by the DGLAP evolution of a parton density. In principle it allows us to "move" PDF's to higher energies and virtualities than that of the deep inelastic scattering. Passing to the NLO order solves most of problems of partonic approach, nevertheless there is a problem that the K factor correction is of the order of 2-3 times the first order and so it can be even larger in further orders. Furthermore, there appears to be a problem with p_T spectrum, because theoretical calculations correspond to $p_T \sim M^2$ and even diverge at $p_T \to 0$

$$\frac{d\sigma}{dp_T^2} \sim \frac{\alpha_S(p_T^2)}{p_T^4} \tag{2.15}$$

That is a consequence of the fact that large logarithms ln $\frac{M^2}{p_T^2}$ occur in high orders of pQCD and therefore they have to be resumed all. It corresponds to a resummation of soft gluons radiated from a quark or antiquark.

Chapter 3

The Drell-Yan process in light cone dipole approach

3.1 The Light cone model cross-section calculation

In the rest frame of a target, the Drell-Yan process looks like a bremsstrahlung of a massive photon from an incoming quark. The photon can be emitted before or after a quark is scattered on a proton[2].

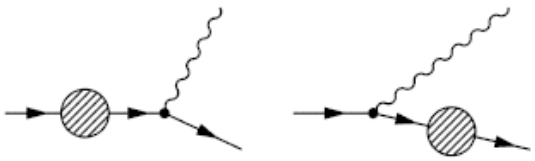

Figure 3.1: The Dell-Yan production via a color dipole approach

This photon then decays into a l^+l^- pair. Although the cross section is a Lorentz invariant variable, the space-time interpretation of a process is not a Lorentz invariant variable and therefore depends on a reference frame. The Feynmann picture of colliding particles seen as a bunch of non-interacting partons without transverse momentum can be used only in a fast moving reference frame (so called infinite momentum frame). Only there the Drell-Yan process can be formulated using parton densities in a proton.
In a rest frame of the target $q/\bar{q}$ a quark from the incident hadron fluctuates to a state that contains massive photon and a quark. Strong interaction with target color field interrupts the coherence of a fluctuation and the photon is

released as virtual. In analogy to the factorization theorem[3]

$$\frac{d\sigma}{dln\alpha}(qp \to \gamma^\star X) = \int d^2\rho |\Psi_{\gamma^\star q}(\alpha,\rho)|^2 \sigma^N_{q\bar{q}}(\alpha\rho, x_2), \tag{3.1}$$

where $\sigma^N_{q\bar{q}}(\alpha\rho, x_2)$ is a dipole cross section from the DIS and $\Psi_{\gamma^\star q}(\alpha,\rho)$ is a light-cone(LC) distribution amplitude,i.e. an amplitude describing a possibility that there exists a $\gamma^\star q$ fluctuation with a transverse separation $\vec{\rho}$ and a relative part of LC momentum of a photon and quark is α or $1-\alpha$ respectively. The photon in a fluctuation can be longitudinally or transversely polarized, therefore we have to distinguish Ψ^T and Ψ^L.

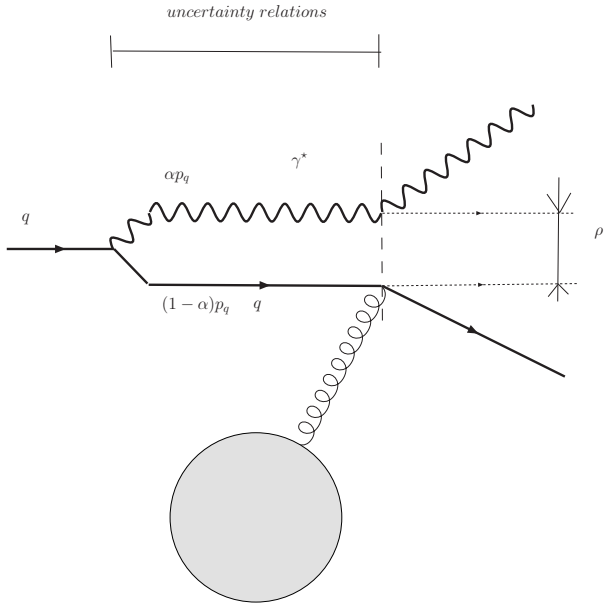

Figure 3.2: A detailed look on a fluctuation propagation and its consecutive disruption

Let's denote

- $P_1 \ldots$ four-momentum of incident beam
- $P_2 \ldots$ four-momentum of a target
- $\vec{q} \ldots$ four-momentum of a virtual photon
- $\vec{q}^T \ldots$ transverse momentum of a virtual photon

Now, similar relations are valid as in parton model, namely

$$s = (P_1 + P_2)^2 \qquad q^2 = M^2 \tag{3.2}$$

Standard kinematical variables are Bjorken x's

$$x_1 = \frac{2P_2.q}{s} \qquad x_2\frac{2P_1.q}{s} \quad x_1x_2 = \frac{M^2+\vec{q}_T^2}{s}, \tag{3.3}$$

connected to a Feynmann variable via

$$x_1 - x_2 = x_F \tag{3.4}$$

The noninvariance of space-time description shows in a way that instead of x_1 be a part of a momentum of incident quark annihilating with an antiquark as in parton model, here x_1 is a part of momentum of proton carried away by photon.
Light-cone wave functions for the Drell-Yan process(DY) can be expressed in analogy with the DIS as[3]

$$\Psi^{T,L}_{\gamma^\star q}(\alpha,\rho) = \frac{\sqrt{\alpha_{em}}}{2\pi}(\bar{\chi}_q\hat{\mathcal{O}}^{T,L}_{\gamma^\star q}\chi_q)K_0(\eta\rho), \tag{3.5}$$

where

$$\begin{aligned}
\eta^2 &= m_f^2\alpha^2 + M^2(1-\alpha)\\
\chi &\ldots 2-\text{component spinor}\\
\hat{\mathcal{O}}^T_{\gamma^\star q} &= im_f\alpha^2\bar{e}(\vec{n}\times\vec{\sigma}) - i(2-\alpha)(\bar{e}.\vec{\nabla}_p) + \alpha\bar{e}(\vec{\sigma}\times\vec{\nabla}_\rho)\\
\hat{\mathcal{O}}^L_{\gamma^\star q} &= 2M(1-\alpha)
\end{aligned}$$

In particular, an exact form can be calculated for a subprocess $q\to\gamma^\star q$

$$\begin{aligned}
|\Psi_{\gamma^\star q}(\alpha,\rho)|^2 &= |\Psi^T_{\gamma^\star q}(\alpha,\rho)|^2 + |\Psi^L_{\gamma^\star q}(\alpha,\rho)|^2 \qquad (3.6)\\
|\Psi^T_{\gamma^\star q}(\alpha,\rho)|^2 &= \frac{\alpha_{em}}{\pi^2}(m_f^2\alpha^4K_0(\eta\rho) + (1+(1-\alpha)^2)\eta^2K_1^2(\eta\rho))\\
|\Psi^L_{\gamma^\star q}(\alpha,\rho)|^2 &= \frac{2\alpha_{em}}{\pi^2}M^2(1-\alpha)^2K_0^2(\eta\rho)
\end{aligned}$$

In order to form a hadronic cross section it is essential to realize that photon carries away a fraction of proton momentum of the magnitude of $x_1 = \frac{\sqrt{x_F^2+4\tau}+x_F}{2}$ and correspondingly a fraction of a quark momentum of the magnitude α.

$$\begin{aligned}
\frac{d\sigma}{dM^2dx_F} &= \frac{\alpha_{em}}{3\pi M^2}\frac{x_1}{x_1+x_2}\int_{x_1}^1\frac{d\alpha}{\alpha^2}\sum_f Z_f^2(q_f(\frac{x_1}{\alpha}) + \hat{q}_f(\frac{x_1}{\alpha}))\frac{d\sigma(qp\to q\gamma^\star p)}{dln\alpha} =\\
&= \frac{\alpha_{em}}{3\pi M^2}\frac{1}{x_1+x_2}\int_{x_1}^1\frac{d\alpha}{\alpha}F_2^p(\frac{x_1}{\alpha})\frac{d\sigma(qp\to q\gamma^\star p)}{dln\alpha} \qquad (3.7)
\end{aligned}$$

The proton structure function needs to be evaluated in quite high x_{Bj}, where it is well known. The existence of "dipole" cross section is well-founded even

if there is no physical dipole. After a quark radiates a photon it is partially inflected in the impact parameter plane. If we denote the transverse separation between a quark and a photon as ρ, then the center of mass of a fluctuation is the same as for the original quark at the impact parameter plane. The distance between photon and the center of mass is exactly $(1-\alpha)\rho$ and an appropriate distance for quark is $\alpha\rho$. The displacement in the coordinate frame leads to a phase factor in the momentum frame.
The incoming quark can be expanded into interaction eigenstates[2]

$$|q>=\sqrt{Z_2}|q_{bare}>+c^q_{\gamma^\star}|q\gamma^\star>+\dots \tag{3.8}$$

Different eigenstates are scattered with different amplitudes, which has an effect of disturbing the coherence amongst eigenstates. Considering the fact, that there is no real dipole in the DY process, the non-perturbative interaction need not to be taken into account. So we stick to perturbative light-cone wave functions. Since the dipole cross section consider only sea quarks from gluon decays, the LC approach to the DY process can be used only for small x_2. That is a reason for the dependence of the dipole cross section on the gluon density. Naturally, the fact whether a sea quark belongs to incident or target quark is frame dependent. If an incident quark or antiquark is "slow" in the infinity momentum frame in the limit $\alpha \to 1$, it can be interpreted as a sea antiquark or quark of a target, that annihilates with an incoming parton. The annihilation of valence quarks of a target was not taken into account.
Let's denote that even if a quark mass is negligible, it cannot be set to zero. Divergencies coming from finite boundaries in α integration lead to logarithmic divergencies in standard approach. The region $\alpha \to 0$ is the analogy of Bjorken aligned jet configurations that lead to a dominant contribution to the p_T distribution. It can be obtained by four-fold Fourier transformation

$$\begin{aligned}\frac{d\sigma(qp\to q\gamma^\star p)}{dln\alpha d^2p_T} &= \frac{1}{(2\pi)^2}\int d^2\rho_1 d^2\rho_2 e^{i\vec{p}_T(\vec{\rho}_1-\vec{\rho}_2)}\Psi^\star_{\gamma^\star q}(\alpha,\rho_1)\Psi_{\gamma^\star q}(\alpha,\rho_2)\times \\ &\times\frac{1}{2}(\sigma_{q\bar{q}}(\alpha\rho_1)+\sigma_{q\bar{q}}(\alpha\rho_2)-\sigma_{q\bar{q}}(\alpha|\vec{\rho}_1-\vec{\rho}_2|)).\end{aligned} \tag{3.9}$$

The LC wave function can be expressed as

$$\begin{aligned}\Psi^{\star T}(\alpha,\rho_1)\Psi^T(\alpha,\rho_2) &= \frac{\alpha_{em}}{\pi^2}(m_f^2\alpha^4K_0(\eta\rho_1)K_0(\eta\rho_2)+ \\ &\quad +(1+(1-\alpha)^2)\eta^2\frac{\vec{\rho}_1\vec{\rho}_2}{\rho_1\rho_2}K_1(\eta\rho_1)K_1(\eta\rho_2)) \\ \Psi^{\star L}(\alpha,\rho_1)\Psi^L(\alpha,\rho_2) &= \frac{2\alpha_{em}}{\pi^2}M^2(1-\alpha)^2K_0(\eta\rho_1)K_0(\eta\rho_2)\end{aligned} \tag{3.10}$$

Final hadronic differential cross section is

$$\frac{d\sigma}{dM^2dx_Fd^2p_T}=\frac{\alpha_{em}}{3\pi M^2}\int_{x_1}^1\frac{d\alpha}{\alpha}F_2^p(\frac{x_1}{\alpha})\frac{d\sigma(qp\to qp\gamma^\star)}{dln\alpha d^2p_T} \tag{3.11}$$

3.2 The Drell-Yan pair polarization

In experiment, different polarizations can be distinguished by the study of angular distribution of DY pairs. In general, the distribution has a form of

$$\frac{d^4\sigma}{dx_F dM^2 d\cos\Theta d\phi} \sim 1 + \lambda\cos^2\Theta + \mu\sin 2\Theta\cos\phi + \frac{\nu}{2}\sin^2\Theta\cos 2\phi \qquad (3.12)$$

Since λ, ϕ depend on a z-axis of the center-of-mass frame of a dilepton, it has to be reformulated to fit the color dipole approach. The formulation of the color dipole approach in the rest frame of a target restrict the z axis to the direction of a radiated photon. Then, the rest frame of a target and the center-of-mass frame of dilepton are connected with a boost in the z axis and therefore transverse polarizations are in both frames the same

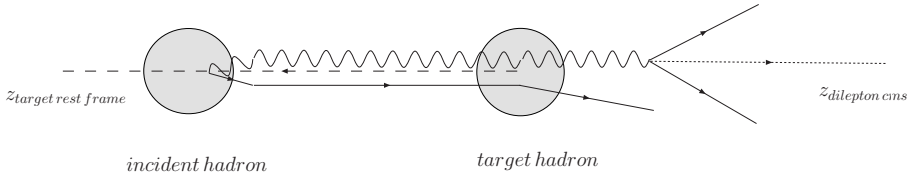

Figure 3.3: A choice of a z axis for the polarization analysis

Since ϕ-dependence is hard to measure, it can be carried out by integrating the whole formula over 2π

$$\frac{d^3\sigma}{dx_F dM^2 d\cos\Theta} \sim 2\pi(1 + \lambda\cos^2\Theta) \qquad (3.13)$$

From the experimental observation it is known that $\lambda = +1$ for transverse and $\lambda = -1$ for longitudinal polarization and then

$$\lambda = \frac{\sigma_T - \sigma_L}{\sigma_T + \sigma_L} \qquad (3.14)$$

For small p_T, λ differs from 1 the more the energy decrease. In opposite, for high p_T, $\lambda \to 1$. In the parton model, the following Lam-Tung relation[12] holds

$$1 - \lambda - 2\nu = 0. \qquad (3.15)$$

This relation, however, does not hold in a color dipole approach. This comes from the behavior of λ in a regime $p_T \to 0$. It is essential that the double-spin-flip amplitude ν vanish at $p_T = 0$ to resolve kinematics. This assumption holds in the first order in pQCD and even in the second order approximately. Experiments suggest that following relation does not hold, but data do not fit proper kinematic region. It is only known experimentally in large x_2, where the

color dipole approach do not count.
The dipole formalism offers easy way to calculate the DY p_T distribution even in low-p_T region. Results from $\mathcal{O}(\alpha_S)$ parton model cannot be directly compared to the color dipole approach since it is not an expansion in any parameter. Instead of this, all contributions from higher order graphs enhanced by factor of $\ln(\frac{1}{x_2})$ are included in the dipole cross section. Using proper phenomenological parametrization there can be even non-perturbative corrections included.

Chapter 4

Phenomenological parametrization

4.1 The dipole cross section

The dipole cross-section parametrization is the most important feature of the whole light cone approach. Since it cannot be calculated directly it has to be extracted from a phenomenology fit to known data. Fortunately, results from the DIS data fits can be used for processes described by the light cone approach[3]. In fact, every hadron cross section can be expressed using the dipole cross section. For example, $\pi - p$ scattering cross section can be written as

$$\sigma_{\pi p}(s) = \int d^2\rho |\Psi_\pi(\rho)|^2 \sigma_{q\bar{q}}(s,\rho). \tag{4.1}$$

The only problem is that we have to be able to calculate $\Psi_\pi(\rho)$, which is a probability of finding a $q\bar{q}$ pair with a transverse separation ρ inside a pion. The general form of a dipole cross-section cannot be calculated as was stated before. But for small ρ it can be expressed using a gluon density in analogy to DGLAP

$$\sigma_{q\bar{q}}(x_{Bj},\rho) = \frac{\pi^2}{3}\rho^2\alpha_S(\frac{\lambda'}{\rho^2})x_{Bj}G(x_{Bj},\frac{\lambda'}{\rho^2}) \tag{4.2}$$

There exist several parametrizations already. The simplest one is

$$\sigma_{q\bar{q}}(s,\rho) = C(s)\rho^2. \tag{4.3}$$

This is just a naive approximation, where the assumption that α_S and G are independent of transverse separation is used. Probably the biggest problem of this parametrization is the fact that it diverges when $\rho \to \infty$ leading to infinite probability of forming a fluctuation large enough.

Based on a saturation model, Golec-Biernat and Wusthoff proposed a parametrization [10]

$$\sigma_{q\bar{q}}(x_{Bj},\rho) = \sigma\left(1 - e^{-\frac{\rho^2 Q_0^2}{4(\frac{x}{x_0})^\lambda}}\right), \tag{4.4}$$

where $Q_0 = 1\text{GeV}$, $\sigma_0 = 23.03\text{mb}$, $x_0 = 0.0003$, $\lambda = 0.288$.

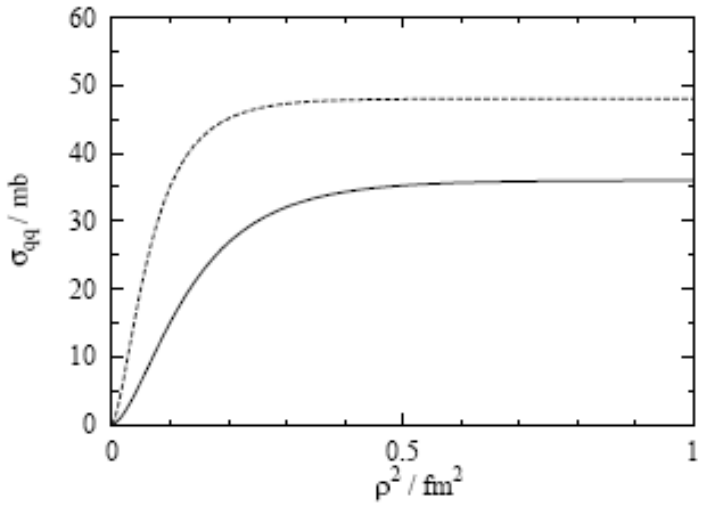

Figure 4.1: The dipole cross-section vs. ρ^2 - solid for HERA, dashed for THERA energy

There can still be a problem because there is no Bjorken variable in hadron-hadron collisions and the energy is "hidden" in s. But if we reformulate the dipole cross-section as a function of s, the Bjorken scaling is automatically violated. A compromise solution is to parametrize the dipole cross-section with $\rho^2 s$, which maintains approximate Bjorken scaling but introduce 10 parameters and restricts a validity up to $Q^2 = 60\text{GeV}^2$. Since we know that the Bjorken scaling is strongly violated at low x_{Bj}, we can reformulate the dipole cross-section using s and restrict to rather low Q^2.

$$\sigma_{q\bar{q}}(s,\rho) = \sigma_0(s)\left(1 - e^{-\frac{\rho^2}{r_0^2(s)}}\right) \tag{4.5}$$

$$r_0(s) = 0.88\left(\frac{s}{s_0}\right)^{-0.14}\text{fm}\,;\; s_0 = 1000\text{GeV}^2$$

$$\sigma_0(s) = \sigma_{tot}^{\pi p}(s)\left(1 + \frac{3r_0^2(s)}{8 < r_{ch}^2 >_\pi}\right)$$

$$\sigma_{tot}^{\pi p}(s) = 23.6 \left(\frac{s}{s_0}\right)^{0.08} \text{mb}\,; < r_{ch}^2 >_\pi = 0.44\text{fm}^2$$

There are several other possibilities how to improve this parametrization. The data agreement can be enhanced by introducing "non-physically" small quark masses. That would, however, allow for arbitrarily large separations of quarks, which breaks a confinement. Masses are therefore selected as an inverse of a typical confinement radius[9]

$$m_{u,d} \sim 200\text{MeV} \tag{4.6}$$

There is even a possibility to include a DGLAP evolution into dipole cross section

$$\sigma_{q\bar{q}}(x_{Bj}, \rho) = \sigma_0 \left(1 - e^{-\frac{\pi^2 \rho^2 \alpha_S(\mu^2) x G(x,\mu^2)}{3\sigma_0}}\right), \tag{4.7}$$

where the scale where we want to evaluate the gluon density is defined as

$$\mu^2 = \frac{C}{\rho^2} + \mu_0^2. \tag{4.8}$$

The gluon density is shifted to a desired scale by using the DGLAP evolution

$$\frac{\partial x g(x,\mu^2)}{\partial \ln \mu^2} = \frac{\alpha_S(\mu^2)}{2\pi} \int_x^1 dz [P_{gq_j}(z,\alpha_S) q_j(\frac{x}{z},\mu^2) + P_{gg}(z,\alpha_S) g(\frac{x}{z},\mu^2)]. \tag{4.9}$$

The initial gluon density is taken at the scale $Q_0^2 = 1\text{GeV}^2$ in the form

$$x g(x,\mu^2) = A_g x^{-\lambda_g} (1-x)^{5.6}, \tag{4.10}$$

where $C = 0.26$, $\mu_0^2 = 0.52\text{GeV}^2$, $A_g = 1.2$ and $\lambda_g = 0.28$. The need for DGLAP evolution is reasonable for extremely high energies corresponding to $x \sim 0.001$

4.2 The Proton structure function

The calculation of production cross-section at hadron colliders relies upon a knowledge of the distribution of the momentum fraction x of partons in proton in the relevant kinematic range. These parton distribution functions are a soft component of the cross section and therefore they cannot be calculated perturbatively, but rather are determined by global fits to data from the deep inelastic scattering. Measurements of deep inelastic scattering structure functions (F_2, F_3) in the lepton-hadron scattering provide the main source on quark distributions $q(x,Q)$ inside hadrons. At LO, the gluon distribution function $g(x,Q)$ enters directly in hadron-hadron scattering processes with jet final states. Recent global parton distribution fits are carried out to the NLO and in some cases

to the NNLO, which allows $\alpha_S(Q^2)$,$q(x,Q)$ and $g(x,Q)$ to mix and contribute in the theoretical formulae for all processes. Data from deep inelastic scattering utilized in PDF fits cover a wide range in x and Q. The accuracy of the extrapolation to higher Q^2 depends on the accuracy of the original measurement, uncertainty on $\alpha_S(Q^2)$ and the accuracy of the evolution code. Most global PDF analysis are carried out at NLO. The DGLAP evolution kernels have been calculated at NNLO and so NNLO PDF's calculated in this manner are available. However, any current NNLO global PDF analysis are still approximative. All global analysis use a generic form for the parametrization of both the quark and gluon distributions at some reference value Q_0

$$F(x,Q_0) = A_0 x^{A_1}(1-x)^{A_2} P(x, A_3 \dots). \tag{4.11}$$

The reference value Q_0 is usually chosen in the range of 1-2GeV. The parameter A_1 is associated with small-x Regge behaviour while A_2 is associated with the large-x valence counting rules. The term $P(x, A_3 \dots)$ is a suitably chosen smooth function, depending on one or more parameters, that adds more flexibility to the pdf parametrization.
There are two sets of distribution functions used in this analysis. First is a fit to data from BCDMS,E665,NMC,SLAC,H1,ZEUS taken form [4]. The F_2 parametrization has a form of

$$F_2^{fit}(x,Q^2) = A(x)\left[\frac{ln(\frac{Q^2}{\Lambda^2})}{ln(\frac{Q_0^2}{\Lambda^2})}\right]^{B(x)}\left[1+\frac{C(x)}{Q^2}\right] \tag{4.12}$$

$$A(x) = x^{a_1}(1-x)^{a_2}[a_3 + a_4(1-x) + a_5(1-x)^2 + a_6(1-x)^3 + a_7(1-x)^4]$$

$$B(x) = b_1 + b_2 x + \frac{b_3}{x+b_4}$$

$$C(x) = c_1 x + c_2 x^2 + c_3 x^3 + c_4 x^4$$

with $Q_0^2 = 20\text{GeV}^2$ and $\Lambda = 0.25$.

Fitting parameters are summarized in [4]. Validity of this parametrization lies in a kinematic range of $0.2 < Q^2 < 5000\text{GeV}^2$ and $3.5\times10^{-5} < x < 0.85$. Since this fit do not cover the whole interval in x, this function is particularly inconvenient for low energy calculations, especially for the DY. But our main objective is to perform this approach towards the ALICE energies, where high-x behaviour do not contribute significantly.
The second parametrization comes from [5], where LO and NLO quarks and gluon distribution functions are presented. For LO they are evaluated at a scale

$$s = \ln\frac{\ln\left[\frac{Q^2}{0.232^2}\right]}{\ln\left[\frac{\mu_{LO}^2}{0.232^2}\right]}, \quad \mu_{LO}^2 = 0.23 \tag{4.13}$$

using a function

$$xv(x,Q^2) = Nx^a(1 + Ax^b + Bx + Cx^{3/2})(1-x)^D \tag{4.14}$$

and parameters for each valence quark mentioned at [5], dependent on s. The gluons and sea quarks parametrization has a form of

$$xw(x,Q^2) = \left[x^a(A + Bx + Cx^2)(\ln(1/x))^b + s^\alpha e^{-E+\sqrt{E's^\beta \ln(1/x)}}\right](1-x)^D. \tag{4.15}$$

Since valence quark u is normalized to 2 and valence quark d to 1, the structure function of a proton is described by

$$xF_2^p(x,Q^2) = Z_u^2 xu_v(x,Q^2) + Z_d^2 xd_v(x,Q^2) + Z_u^2 2xu_s(x,Q^2) + Z_d^2 2xd_s(x,Q^2), \tag{4.16}$$

where Z_u and Z_d are electric charges of appropriate quarks. The validity lies in a region of $0.4 < Q^2 < 10^6 GeV^2$ and $10^{-5} < x < 1$.
The only difference between LO and NLO paramatrizations lies in a fact that NLO is evaluated with other parameters[5] at the scale

$$s = \ln\frac{\ln\left[\frac{Q^2}{0.248^2}\right]}{\ln\left[\frac{\mu^2_{NLO}}{0.248^2}\right]}, \quad \mu^2_{NLO} = 0.34 \tag{4.17}$$

The validity remains the same.

4.3 The Deuteron structure function

The deuteron structure function can be either extracted from the DIS directly or composed from quark and gluon structure functions. The latter has a disadvantage in the fact hat it neglects collective effects even if they are not as strong.
The first deuteron structure function used in this analysis comes from [4]. This global fit to BCDMS,E665,NMC ans SLAC data gives a stand-alone function for a whole deuteron. Explicit form of this function is the same as for a proton with different set of parameters, mentioned in [4]. A validity region is $0.2 < Q^2 < 220 GeV^2$ and $0.0009 < x < 0.85$.
The second deuteron structure function is constructed from quark and gluon structure functions taken from [5] as in case of a proton. The fact that each quark distribution is normalized to a different value is manifested in different coefficients beside each distribution.

$$xF_2^p(x,Q^2) = Z_u^2(\frac{3}{2})xu_v(x,Q^2) + Z_d^2(3)xd_v(x,Q^2) + Z_u^2 4xu_s(x,Q^2) + Z_d^2 4xd_s(x,Q^2), \tag{4.18}$$

Validity region is the same as for a proton.

Chapter 5

Transition from p-p to p-A(d-A) collisions

5.1 The parton model calculation

As it was said before, using the DIS data for p-p collisions one cannot make reasonable generalization for the DY process to p-A or A-A collisions. Nuclear effects are described by a quantity named the nuclear modification factor

$$R_{DY}^{pA}(x_1,x_2)=\frac{\sigma_{DY}^{pA}(x_1,x_2)}{A\sigma_{DY}^{NN}(x_1,x_2)} \qquad R_{DY}^{AB}(x_1,x_2)=\frac{\sigma_{DY}^{AB}(x_1,x_2)}{AB\sigma_{DY}^{NN}(x_1,x_2)} \tag{5.1}$$

If we use a cross-section calculation from chapter 2, the nuclear generalization would look like[2]

$$\begin{aligned}\sigma_{DY}^{pA}(x_1,x_2) &= N\sum_f Z_f^2\int d^2bT_A(\vec{b})\Big(\underbrace{q_f^v(x_1)R_s^A(x_2,\vec{b})\bar{q}_f^s(x_2)}_{\text{annihilation of } q_v^p \text{ with } q_s^A}+\\ &\bar{q}_f^s(x_1)R_v^A(x_2,\vec{b})q_f^v(x_2)+q_f^s(x_1)R_s^A(x_2,\vec{b})\bar{q}_f^s(x_2)+\\ &\bar{q}_f^s(x_1)R_s^A(x_2,\vec{b})q_f^s(x_2)+\underbrace{val-val}_{\text{strongly suppresed}}\Big)\end{aligned} \tag{5.2}$$

$$\sigma_{DY}^{AB}(x_1,x_2) = N\sum_f Z_f^2 \int d^2b \int d^2s T_A(\vec{s})T_B(\vec{b}-\vec{s}) \tag{5.3}$$

$$\Big(\underbrace{q_f^v(x_1)R_v^A(x_1,\vec{s})\bar{q}_f^s(x_2)R_s^B(x_2,\vec{b}-\vec{s})}_{\text{annihilation of } q_v^A \text{ with } q_s^B} +$$
$$+\bar{q}_f^s(x_1)R_s^A(x_1,\vec{s})q_f^v(x_2)R_v^B(x_2,\vec{b}-\vec{s}) +$$
$$+q_f^s(x_1)R_s^A(x_1,\vec{s})\bar{q}_f^s(x_2)R_s^B(x_2,\vec{b}-\vec{s}) +$$
$$+\bar{q}_f^s(x_1)R_s^A(x_1,\vec{s})q_f^s(x_2)R_s^B(x_2,\vec{b}-\vec{s}) +$$
$$+ \underbrace{val-val}_{\text{strongly suppresed}} \Big) \tag{5.4}$$

$$\sigma_{DY}^{NN}(x_1,x_2) = N\sum_f Z_f^2\Big(q_f^v(x_1)\bar{q}_f^s(x_2)+\bar{q}_f^s(x_1)q_f^v(x_2)+$$
$$+q_f^s(x_1)\bar{q}_f^s(x_2)+\bar{q}_f^s(x_1)q_f^s(x_2)\Big) \tag{5.5}$$

All parton distributions q_f are taken at the same virtuality $Q^2 = M^2$. The $R_q^A(x,b)$ is a function of the impact parameter for small x. It reaches maximum for $b = 0$(central collision) and vanishes as $b \to R_A$. However, data from the deep inelastic scattering in p-A collisions provide only information about $\int d^2bR_q^A(x,\vec{b})$ and therefore the calculation cannot be performed. Nevertheless, there was introduced an ad-hoc assumption that $R_q^A \backsimeq b$ in a parton model. But as was stated earlier, that is in direct contradiction with the experiment because it leads to the situation when nuclear shadowing is independent of a centrality.

5.2 The p-A cross-section calculation

Naively, one can assume that the transition from a proton target to a nuclear target leads to A times a p-p cross-section. But as was seen from experiments, nuclear effects have quite strong influence on a final cross-section. For middle x_{Bj} the ratio $\frac{\sigma^A}{A\sigma^N}$ resp. $\frac{F^A}{AF^N}$ is suppressed due to the EMC effect. In the region around $x_{Bj} \sim 0.1$, the ratio is enhanced due to a nuclear anti-shadowing. For extremely small values of x_{Bj}, there is a permanent decrease due to a nuclear shadowing[3].

In order to cross from p-p collisions to p-A collision it is necessary to adapt the cross-section calculation properly. In a light cone approach it is quite easy to do so. That is because it do not separate a hard and a soft component but rather separate subprocesses from each other. It is therefore easy to change the part corresponding to the interaction of a quark with a nucleon for a part

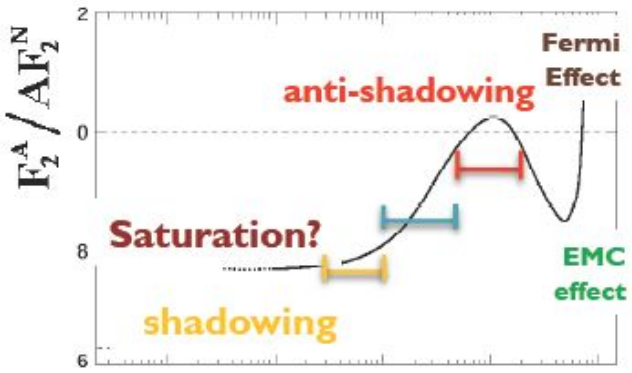

Figure 5.1: The dependence of nuclear effects on the energy scale for several elements

describing the interaction of a quark with a nucleus. The basic assumption is that the coherence time is long enough ($t_c >> R_A$) and so the fluctuation can pass through the whole nucleus without loosing coherence. This is fully met at energies corresponding to $x \sim 0.1$. In this limit, the incoming quark can be dissolved to a system of Fock states with a constant transverse separation $\vec{\rho}$. Since parton configurations with a constant transverse separation in an impact parameter space constitute eigenstates of an interaction, the σ^A can be calculated using the eikonalization of σ^N(Glauber theory)[13]

$$\sigma^A_{q\bar{q}}(\rho, x) = 2 \int d^2b \left(1 - (1 - \frac{1}{2A}\sigma^N_{q\bar{q}}(\rho, x) T_A(b))^A\right), \tag{5.6}$$

where A is a mass number of a nucleus. The nuclear thickness T_A can be expressed as

$$T_A(b) = \int_{-\infty}^{+\infty} dz \rho_A(b, z), \tag{5.7}$$

where ρ_A is a nuclear density, parametrized with for example Woods-Saxon approximation. For detailed derivation see appendices. In order to use this approach for high energies, contributions from higher Fock states have to be included. A term corresponding to 1 scattering can be extracted from a Glauber cross section by expanding to the first order in σ^N. A dipole interacts with a target by the exchange of a colorless gluonic system(=pomeron)[2].

The unitarity cut of the amplitude creates a multiple gluon radiation and therefore higher Fock states. This shows that for a single scattering σ^N takes into account all Fock states of an incoming parton. The energy dependence of σ^N is then generated by the phase space of gluons from higher Fock states $|q\bar{q}G>, |q\bar{q}GG> \ldots$

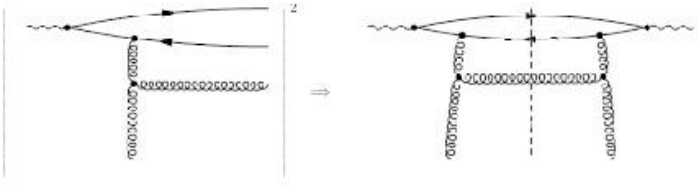

Figure 5.2: Single scattering of higher Fock state

For multiple scattering terms, we can again use the fact that $\sigma^N_{\gamma^\star q} = \sigma^N_{q\bar{q}} = \sigma^N_{DIS}$. The n-times scattered dipole will provide n pomeron ladders.

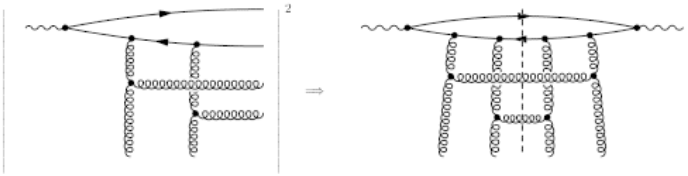

Figure 5.3: Multiple scattering of higher Fock state

That idea leads to a gluon radiation in Bethe-Heitler regime, when each interaction leads to the independent radiation of gluons. But there exist a Landau-Pomeranchuk-Migdal effect(LPM), that point to the fact that the gluon radiation is suppressed, because quark doesn't have enough time to recreate its color field in order to radiate again. This is discussed in more details in the section about a nuclear shadowing.
As the energy rises, the lifetime of this states can become long enough to rescatter a gluon on the nucleon.

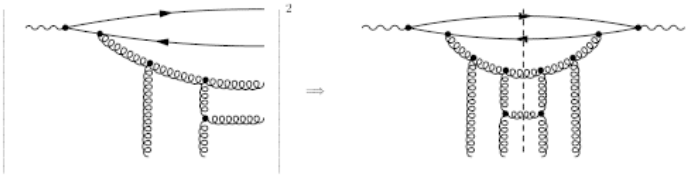

Figure 5.4: Multiple scattering of higher Fock state in the limit of long coherence time - gluon scattering

Such processes lead to a reduction of a gluon density G_A, because two pomerons from the target nucleon merge into one just before the interaction with a fluctuation. As a consequence, the nuclear cross-section is further suppressed. Merging of two pomerons can be included into our calculations by substituting $\sigma^N_{q\bar{q}}$ with $R_G\sigma^N_{q\bar{q}}$, where R_G is a gluon shadowing ratio

$$R_G(x,Q^2) = \frac{G_A(x,Q^2)}{AG_N(x,Q^2)} = 1 - \Delta R_G(x,Q^2) \tag{5.8}$$

Substituting into Glauber cross-section, one obtains

$$\begin{aligned} \sigma^A_{q\bar{q}}(x,\rho) &= 2\int d^2b(1+(1-\frac{A}{2A}\sigma^N_{q\bar{q}}R_G(x,Q^2,b)T_A(b)+\dots)) = \\ &= A\sigma^N_{q\bar{q}}[1-\frac{1}{A}\int d^2b\Delta R_G T_A] + \mathcal{O}((\sigma^N_{q\bar{q}})^2)+\dots \end{aligned} \tag{5.9}$$

Final formula is then

$$\sigma^A_{q\bar{q}}(\rho,x) = 2\int d^2b\left(1-(1-\frac{1}{2A}\sigma^N_{q\bar{q}}(\rho,x)R_G(x,\frac{\lambda}{\rho^2},b)T_A(b))^A\right). \tag{5.10}$$

A Fock state $|q\bar{q}G>$ leads to a multipomeron fusion of a type $nIP \to IP$. But fusions of a type $nIP \to mIP$, corresponding to a Fock state $|q\bar{q}mG>$ is not included. Therefore we perform a summation over m for all processes of a type $nIP \to IP$ to describe $nIP \to mIP$. That is under assumption that each gluon in a state $|q\bar{q}mG>$ reacts to multiple scattering independently on other gluons. This is called Gribov's interpretation of a Glauber eikonal shadowing. The gluon shadowing factor can be calculated using LC Green functions. We restrict ourselves on a shadowing of $|q\bar{q}G>$ state of longitudinally polarized photon. All $q\bar{q}$ dipoles from longitudinal photons have a dimension of $\frac{1}{Q^2}$ and so a gluon can propagate on a long distance from the dipole. Furthermore, the $q\bar{q}$ dipole is in a color-octet state after radiation of a gluon and the whole state looks like a GG dipole. A crucial for the calculation of the gluon shadowing is to determine the distance that gluon can propagate from the quark dipole in the impact parameter space. Diffraction experiments show that a mean dipole size is of the order $r_0 \sim 0.3fm$. Such small gluon cloud around valence quarks is incorporated into the LC wave function by the means of the non-perturbative gluon interaction. A small size of GG dipole leads to quite small gluon suppression. For most values of x, gluon shadowing rises with the thickness of a medium. For medium $x \sim 0.01$, the gluon shadowing is very small and do not need to be taken into account. For LHC energies $x \sim 10^{-5}$ the factor has to be extracted somehow.

5.3 The d-A cross-section calculation

For the purpose of extending the calculation from p-A to d-A collisions, it is necessary to change the structure function of a proton with the structure function

of a deuteron. The dipole cross-section σ^{pA} can be used for d-A calculation, because it is independent of incident particle and describes only the interaction of a dipole with a target medium. The nuclear modification factor for d-A collisions should be suppressed in contrast to the p-A factor, due to stronger influence of valence quarks and isospin effect.

Chapter 6

Nuclear effects on cross section

6.1 Nuclear shadowing

6.1.1 The Parton model description

A partonic interpretation of the shadowing depends on a reference frame. In the infinite momentum frame, the shadowing occurs due to a partonic fusion that leads to a reduction of the partonic density in the low-x_{Bj} region. In the Drell-Yan process, the incoming quark interacts with the microstructure of proton. That, however, cannot be done at infinitely short time. Uncertainty relations tell us, that the bigger the colliding energy is, the longer the interaction takes. In the parton model, energy is substituted by x_{Bj} and time is substituted by $\ln \frac{1}{x_{Bj}}$ in the DGLAP equation

$$\frac{\partial^2 x_{Bj} G(x_{Bj}, Q^2)}{\partial \ln \frac{1}{x_{Bj}} \partial \ln Q^2} = \frac{N_c \alpha_s}{\pi} x_{Bj} G(x_{Bj}, Q^2) \tag{6.1}$$

For fixed α_s the solution behaves asymptotically as[3]

$$x_{Bj} G(x_{Bj}, Q^2) \sim e^{2\sqrt{\frac{N_c \alpha_s}{\pi} \ln \frac{1}{x_{Bj}} \ln \frac{Q^2}{Q_0^2}}} \tag{6.2}$$

Since fast moving nucleus is heavily contracted, parton clouds that carry only small part of a momentum are contracted far less. Therefore, clouds start to overlap. As the energy rises, the gluon density starts to move up and partons start to interact with each other. Using processes like $GG \to G$ or $GG \to q\bar{q}$ the parton density of a nucleus is reduced in contrast with the parton density of free protons. However, this explanation leads to the value of the shadowing dependent only on energy, not the centrality of the collision. It is even independent of the process that takes place, because it is only a feature of a Lorentz contraction.

6.1.2 The Color dipole analysis

In the case of a fixed target frame, the naive interpretation is that incoming quark undergoes several scattering and produce the bremsstrahlung every time it hits a nucleon. But in classical electrodynamics, Landau and Pomeranchuk[15] derived, that the cross-section of bremsstrahlung production by a high-energy charged particle in an amorphous medium is strongly suppressed. A quantum mechanical version of this effect is known as Landau-Pomeranchuk-Migdal(LPM) effect[16]. For low x_2, the multiple scattering of a quark in a nucleus leads to the LPM suppression of a quark bremsstrahlung[2]. This effect is responsible for nuclear shadowing for the DY process. The explanation lies in a fact that quark needs quite a long time to recreate its electromagnetic field after producing a bremsstrahlung. This coherence time(length) goes from uncertainty relations

$$l_c = \frac{1}{q_L} = \frac{\alpha(1-\alpha)E_q}{(1-\alpha)M^2 + \alpha^2 m_f^2 + p_T^2}. \tag{6.3}$$

If a quark is "hit" during this time again, it cannot radiate another photon. Furthermore, it is obvious that Fourier components with high-p_T can radiate sooner than low-p_T and as a consequence are less shadowed. High-p_T corresponds to a narrow fluctuation and low-p_T corresponds to a wide fluctuation. There is a visual analogy to this description. In the nuclear target, a set of nucleons vie for which will release a photon. If a fluctuation has a small transverse size, it can travel through the whole nucleus without breaking the coherence, because there isn't any nucleon that can provide a p_T-kick big enough to break it. Since all nucleons have equal probability to interact, the shadowing is weak.

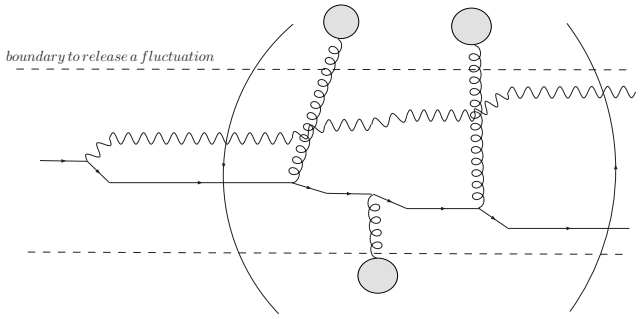

Figure 6.1: A passage of a fluctuation through a nucleus in the short coherence time limit

If a fluctuation is wide enough, only a small impulse is needed to release a photon. Therefore, the coherence of a fluctuation is broken in the first scattering on the surface of a nucleus and it cannot radiate again till the end of a nucleus. That is why nucleons deep in the nucleus do not give significant contribution to the probability of releasing a photon and so they are shadowed by surface

nucleons. Moreover, for high energy experiments the fluctuation with long coherence time do not need to take into account the energy loss. The dilepton is not affected by energy losses of a quark and so the suppression is only due to a shadowing. For low energy experiments the fluctuation is short and the suppression of the cross-section is due to the combination of the shadowing and energy losses of a quark before it fluctuates.
Since photon carries a portion x_1 of proton momentum, the coherence length for the DY can be expressed as

$$l_c = \frac{1}{m_N x_2} \frac{(1-\alpha)M^2}{(1-\alpha)M^2 + \alpha^2 m_f^2 + p_T^2}. \tag{6.4}$$

The role of x_{Bj} from the DIS has a variable x_2 here. As for small x_{Bj} in the DIS the coherence length for the DY can extend the radius of a nucleus for low x_2. In the limit $l_c \to +\infty$ the whole nucleus behaves as one scattering center and the Glauber approximation can be used. Therefore, the partonic cross-section can be expressed in LC factorized form[2]

$$\frac{d\sigma}{dln\alpha}(qA \to \gamma^\star X) = \int d^2\rho |\Psi_{\gamma^\star q}(\alpha,\rho)|^2 \sigma^A_{q\bar{q}}(\alpha\rho, x_2), \tag{6.5}$$

$$\sigma^A_{q\bar{q}}(\rho, x) = 2\int d^2b \left(1 - (1 - \frac{1}{2A}\sigma^N_{q\bar{q}}(\rho, x) T_A(b))^A\right) \tag{6.6}$$

The eikonal term leads to a reduction of a cross-section since it contains the LPM suppression. For a finite coherence length, the DY cross-section is determined using the Green function technique(see Appendices)

$$\frac{d\sigma(qA \to \gamma^\star X)}{dln\alpha} = A\frac{d\sigma(qp \to \gamma^\star X)}{dln\alpha} - Re\int d^2b \int_{\mathbb{R}} dz_1 \int_{z_1}^{+\infty} dz_2 \int d^2\rho_1 \int d^2\rho_2$$
$$(\Psi_{\gamma^\star q}(\alpha,\rho_2))^\star \rho_A(b,z_2)\sigma_{q\bar{q}}(s,\alpha\rho_2) G(\rho_2,z_2|\rho_1,z_1)\rho_A(b,z_1)\sigma_{q\bar{q}}(s,\alpha\rho_1)\Psi_{\gamma^\star q}(\alpha,\rho_1),$$

where the Green function G fulfils a 2D Schrödinger equation

$$\left(i\frac{\partial}{\partial z_2} + \frac{\Delta_\perp(\rho_2) - \eta^2}{2E_q\alpha(1-\alpha)} + \frac{i}{2}\rho_A(b,z_2)\sigma_{q\bar{q}}(s,\alpha\rho_2)\right) G(\rho_2,z_2|\rho_1,z_1) =$$
$$= i\delta(z_2 - z_1)\delta^2(\vec{\rho}_2 - \vec{\rho}_1) \tag{6.7}$$

The phase factor $e^{-iq_L^{min}(z_2-z_1)}$ is implicated in the Green function[3]. Hadronic cross-sections are then

$$\frac{d\sigma^{pp}}{dM^2 dx_F} = \frac{\alpha_{em}}{3\pi M^2}\int_{x_1}^1 \frac{d\alpha}{\alpha} F_2^p(\frac{x_1}{\alpha}) \frac{d\sigma(qp \to qp\gamma^\star)}{dln\alpha}$$
$$\frac{d\sigma^{pA}}{dM^2 dx_F} = \frac{\alpha_{em}}{3\pi M^2}\int_{x_1}^1 \frac{d\alpha}{\alpha} F_2^p(\frac{x_1}{\alpha}) \frac{d\sigma(qA \to qp\gamma^\star)}{dln\alpha d^2p_T}$$

The same is applied to d-A collisions, except that we exchange the F_2^p for F_2^d. Furthermore, we have to neglect nuclear effects in the deuteron structure function, assume the isospin symmetry and neglect finite dimensions effect. The shadowing is described by nuclear modification factors

$$R^{pA} = \frac{\frac{d\sigma(pA\to l^+l^-X)}{dM^2dx_F}}{A\frac{d\sigma(pp\to l^+l^-X)}{dM^2dx_F}} \tag{6.8}$$

$$R^{dA} = \frac{\frac{d\sigma(dA\to l^+l^-X)}{dM^2dx_F}}{2A\frac{d\sigma(pp\to l^+l^-X)}{dM^2dx_F}} \tag{6.9}$$

6.1.3 The Shadowing in A-A collisions

For the determination of the shadowing in more complicated in A-A collisions, it is essential to extend our view. In the σ^{AB}, there appears nuclear shadowing for sea and valence quarks. They have to be evaluated in order to extend the calculation. The shadowing for sea quarks can be extracted from the DIS using a Glauber approximation[2].

$$R_s(x,Q^2,b) = \tag{6.10}$$
$$= \frac{2\int_0^1 d\alpha \int d^2\rho |\Psi_{q\bar{q}}(\rho,\alpha,Q^2)|^2(1-(1-\frac{1}{2A}\sigma^N_{q\bar{q}}(\rho,x)R_G(x,\frac{\lambda}{\rho^2},b)T_A(b))^A)}{T_A(b)\int_0^1 d\alpha\int d^2\rho|\Psi_{q\bar{q}}(\rho,\alpha,Q^2)|^2\sigma^N_{q\bar{q}}(\rho,x)}$$

This expression is valid only in a "frozen approximation", i.e. $t_c >> R_A$ resp. $x \to 0$. The shadowing for valence quarks was presumed to be negligible. The formula for R_s is valid only for gluons since $\sigma^N_{q\bar{q}}$ contains only a part that grows with energy and corresponds to a gluon exchange. Therefore the color dipole approach can be used only for $x < 0.01$, where gluons dominate amongst sea particles. This part of the dipole cross-section is called a pomeron. In the same sense, the valence part corresponds to the reggeon. That is

$$\sigma^N_{q\bar{q}}(\rho,x) = \underbrace{\sigma^{\mathbf{IP}}_{q\bar{q}}(\rho,x)}_{gluonic\,part} + \underbrace{\sigma^{\mathbf{IR}}_{q\bar{q}}(\rho,x)}_{valence\,part} \tag{6.11}$$

The valence part has to correspond to the distribution of valence quarks in a proton for small x

$$\sigma^{\mathbf{IR}} = N\rho^2\sqrt{x}. \tag{6.12}$$

Using this expression we can write

$$R_v(x,Q^2,b) = \tag{6.13}$$
$$= \frac{\int_0^1 d\alpha\int d^2\rho|\Psi_{q\bar{q}}(\rho,\alpha,Q^2)|^2\sigma^{\mathbf{IR}}_{q\bar{q}}(\rho,x)(1-\frac{1}{2A}\sigma^{\mathbf{IP}}_{q\bar{q}}(\rho,x)R_G(x,\frac{\lambda}{\rho^2},b)T_A(b))^A}{\int_0^1 d\alpha\int d^2\rho|\Psi_{q\bar{q}}(\rho,\alpha,Q^2)|^2\sigma^{\mathbf{IR}}_{q\bar{q}}(\rho,x)}$$

6.2 Nuclear broadening

The last thing to discuss is how the nuclear medium will influence the p_T distribution of the DY pair. The full formula for the p_T distribution is

$$\begin{aligned}\frac{d^3\sigma^{qA}}{d\ln\alpha d^2p_T} &= \frac{\alpha_{em}}{(2\pi)^4 4E_q^2(1-\alpha)^2}2Re\int_{\mathbb{R}}dz_1\int_{z_1}^{+\infty}dz_2\int d^2bd^2k_Td^2\rho_1d^2\rho_2 \\ &e^{\left(i\alpha\vec{p}_2\vec{\rho}_2-i\alpha\vec{p}_1\vec{\rho}_1-i\int_{z_2}^{+\infty}dzV_{opt}(b,\rho_2,z)-i\int_{-\infty}^{z_1}dzV_{opt}(b,\rho_1,z)\right)} \\ &\hat{O}^{\star}_{\gamma^\star q}(\rho_2)\hat{O}_{\gamma^\star q}(\rho_1)G(\rho_2z_2|\rho_1z_1). \end{aligned} \tag{6.14}$$

We will introduce the transverse momentum of the incident quark in respect to the direction of a virtual photon

$$\vec{p}_1 = \frac{\vec{p}_T}{\alpha} \tag{6.15}$$

and the transverse momentum of the outgoing quark with same conditions

$$\vec{p}_2 = \vec{k}_T - \frac{(1-\alpha)\vec{p}_T}{\alpha}. \tag{6.16}$$

The interaction with the nuclear medium is incorporated in the Green function and the optical potential[3]

$$V_{opt}(b,\rho,z) = -\frac{i}{2}\rho_A(b,z)\sigma_{q\bar{q}}(s,\rho). \tag{6.17}$$

In the limit of infinite energy of the incoming quark, the cross-section can be expressed as

$$\begin{aligned}\frac{d^3\sigma^{qA}}{d\ln\alpha d^2p_T} = \frac{1}{(2\pi)^2}\int d^2\rho_1d^2\rho_2e^{i\vec{p}_T(\vec{\rho}_1-\vec{\rho}_2)}\Psi^{\star}_{\gamma^\star q}(\alpha,\rho_1)\Psi_{\gamma^\star q}(\alpha,\rho_2) \\ \frac{1}{2}(\sigma^A_{q\bar{q}}(\alpha\rho_1)+\sigma^A_{q\bar{q}}(\alpha\rho_2)-\sigma^A_{q\bar{q}}(\alpha(\rho_1-\rho_2)))\end{aligned} \tag{6.18}$$

where as $\sigma^A_{q\bar{q}}$ the Glauber formula is taken(see 5.6).

Let's see moments of this distribution. Broadening can be displayed on the mean value of p_T^2

$$\delta < p_T^2 > = < p_T^2 >_A - < p_T^2 >_N \tag{6.19}$$

$$< p_T^2 >_A = \frac{\int_0^{p_T^{max}} d^2p_Tp_T^2\frac{d\sigma^{pA}}{d^2p_T}}{\int_0^{p_T^{max}} d^2p_T\frac{d\sigma^{pA}}{d^2p_T}} \tag{6.20}$$

The mechanism behind this phenomenon can be expressed qualitatively. It is essential to distinguish short coherence time fluctuations and long time fluctuations. For short t_c the hard fluctuation is created inside the nucleus and is

immediately split. Before fluctuating, the quark can have soft interactions in the initial state. That will not produce lepton pairs, but it will raise the mean p_T. The fast parton undergoes several interactions and provide something like a Brownian motion in the transverse plane.

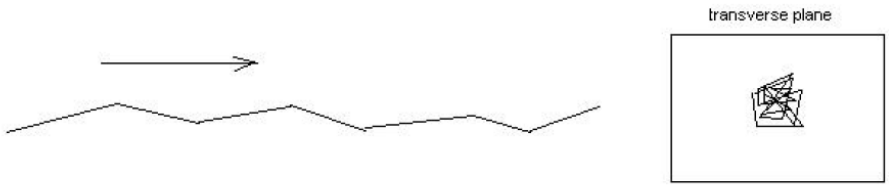

Figure 6.2: The Brownian motion of a quark passing through the medium - nuclear broadening in the limit of a short coherence time

Finally, a quark reaches the hard interaction region, where the DY pair is created, with different p_T than at the beginning. This difference will pass over to the photon and consequently to the dilepton. Therefore, the p_T distribution is wider for p-A than for p-p case. This situation cannot be described using a standard parton approach by modifying quark distribution functions.
For a long coherence time, the explanation is different. The high-energy incident quark evolve to a fluctuation long before the nucleus. A photon and a quark in the fluctuation cannot influence each other due to the time dilatation. Therefore, the broadening cannot come from multiple interactions of a quark in the nucleus. But one can see, that not all fluctuations contribute to the DY pair production equally. The smaller the fluctuation is(=bigger intrinsic relative p_T between quark and dilepton) the bigger "kick" in the p_T plane from the target nucleon is needed for loosing the coherence. Big fluctuations with small intrinsic p_T will with high probability loose the coherence during the first scattering. In contrast to one scattering on a nucleon target, multiple scattering inside the nucleus can split smaller fluctuations.

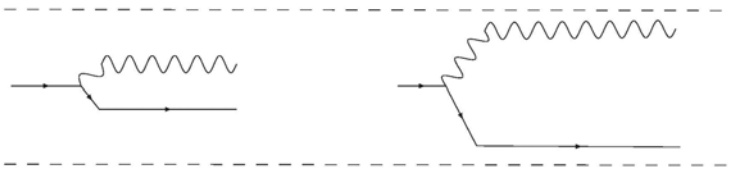

Figure 6.3: Contributions of different fluctuations to a p_T spectrum - nuclear broadening in the limit of long coherence time

This mechanism prefer DY pairs with "middle" p_T. In high-p_T only one scattering dominates and the enhancement of the production do not come. The p_T distribution then widens again. This mechanism is called a color filtering. The enhancement in the region above 1GeV is called Cronin effect. The specific value of a broadening depend on the maximal p_T we use for the analysis. The same feature can be seen in experimental data.
Nuclear broadening and nuclear shadowing are deeply connected. It can be shown that when there is one of them, there is also the second present[2].

$$\frac{\int_0^{p_T^{max}\to+\infty} d^2p_T p_T^2 \frac{d\sigma^{pA}}{d^2p_T}}{\int_0^{p_T^{max}\to+\infty} d^2p_T \frac{d\sigma^{pA}}{d^2p_T}} = \eta^2 + \frac{C^A(x_2)}{\sigma^{qA}(\alpha)} \int d^2\rho |\Psi_{\gamma^\star q}(\alpha,\rho)|^2 \tag{6.21}$$

$$\eta^2 = (1-\alpha)M^2 + \alpha^2 m^2 \quad ; \quad \sigma^{qA}(\alpha) = \int d^2p_T \sigma^{qA}(p_T,\alpha) \tag{6.22}$$

$$C^A(x_2) = \frac{\partial \sigma^A_{q\bar{q}}(\rho,x_2)}{\partial \rho^2}\Big|_{\rho\to 0} \tag{6.23}$$

If we include shadowing, then

$$C_A(x_2) = C^N(x_2) \int d^2b R_G(x_2,b) T(b) = C^N(x_2)(A - \int d^2b \Delta R_G(x_2,b) T(b)) \tag{6.24}$$

$$\Rightarrow \quad \delta < p_T^2 >= (\Delta R_{DY} - \frac{1}{A} \int d^2b \Delta R_G(x_2,b) T(b)) \frac{A C^N(x_2)}{\sigma^{qA}(\alpha)} \int d^2\rho |\Psi_{\gamma^\star q}(\alpha,\rho)|^2, \tag{6.25}$$

where ΔR_{DY} is a nuclear suppression for DY pairs and ΔR_G is a nuclear suppression for gluons. Therefore, if we want non-zero broadening, we need the shadowing for quarks and gluons. The cut-off p_T^{max} is hidden in the integral of $|\Psi|^2$. The need of this cut-off corresponds to the maximal acceptance of the detector where the p_T distribution is measured. Using several approximations, the formula can be further simplified. The wave function distribution can be substituted by a Gaussian

$$|\Psi(\alpha,\rho)|^2 \to \frac{\alpha_{em}}{2\pi}(1+(1-\alpha)^2)\eta^2 n^2 e^{-k_0^2\rho^2} \quad k_0^2 = 2\beta\eta^2, \tag{6.26}$$

where n^2 and β are parameters. Then

$$\begin{aligned}
\int d^2p_T p_T^2 \frac{d\sigma^{pA}}{d\ln\alpha d^2p_T} &= \int d^2p_T p_T^2 \frac{1}{(2\pi)^2}\int d^2\rho_1 d^2\rho_2 e^{ip_T(\rho_1-\rho_2)}\Psi^\star(\alpha,\rho_1)\Psi(\alpha,\rho_2) \\
&\quad \frac{1}{2}(\sigma^A_{q\bar{q}}(\alpha\rho_1,x_1)+\sigma^A_{q\bar{q}}(\alpha\rho_2,x_2)-\sigma^A_{q\bar{q}}(\alpha|\rho_1-\rho_2|,x_2)) = \\
&= \pi\int d^2b(\frac{2C(\alpha)\alpha^2T_A(b)}{k_0^2}+\frac{2(C(\alpha)\alpha^2T_A(b))^2}{(2k_0^2+C(\alpha)\alpha^2T_A(b))^2}) = \\
&= \pi\int d^2b(\frac{2C(\alpha)\alpha^2T_A(b)}{k_0^2}+\frac{(C(\alpha)\alpha^2T_A(b))^2}{k_0^4}+\dots) \\
\int d^2p_T \frac{d\sigma^{pA}}{d\ln\alpha d^2p_T} &= \pi\int d^2b(\frac{C(\alpha)\alpha^2T_A(b)}{k_0^4}+\frac{(C(\alpha)\alpha^2T_A(b))^2}{k_0^6}+\dots)
\end{aligned}$$

For the proper choice of parameters n and β the following conditions have to hold:

- $\int_0^{+\infty}\rho^2K_1^2(\eta\rho)d^\rho = n^2\int_0^{+\infty}\rho^2e^{-k_0\rho^2}d^2\rho \Rightarrow n^2=\frac{16\beta}{3}$
- We set β so that $<\rho^2>$ remains the asymptotic form of $K_1(x)\Rightarrow\ \beta=1$

Using these conditions, the result is $p_T^{max}\sim 10\text{GeV}$[2].
In the limit, where $t_c\to 0$, the broadening rises linearly with the path it travels in the nuclear medium before the DY pair is released.

$$\delta<p_T^2>_q = C(x_2)<T_A>=C(x_2)\int d^2b\frac{T_A^2(b)}{A} \tag{6.27}$$

After a dilepton is released, the broadening can be written as

$$\delta<p_T^2>_{DY}=<\alpha^2>\delta<p_T^2>_q, \tag{6.28}$$

where

$$<\alpha^2>=\frac{\int_0^1 d\alpha\alpha^2\int d^2\rho|\Psi_{q\gamma^\star}(\rho,\alpha,M^2)|^2\sigma^N_{q\bar{q}}(\rho,x)}{\int_0^1 d\alpha\int d^2\rho|\Psi_{q\gamma^\star}(\rho,\alpha,M^2)|^2\sigma^N_{q\bar{q}}(\rho,x)} \tag{6.29}$$

is a fraction of momentum of a quark that goes to the DY pair.
Now, we are in the situation when we have two expressions in each kinematical regime. In the long coherence time regime, if we expand the $\sigma^A_{q\bar{q}}$ in $\sigma^N_{q\bar{q}}T_A(b)$, then the integration over the longitudinal part of a light-cone wave function can be performed analytically(the transverse part diverges) and the broadening can be written as

$$\delta<p_T^2>_{t_c>>R_A}=KC(x_2)\int d^2b\frac{T_A(b)}{A} \tag{6.30}$$

$$K=\frac{<(\sigma^N_{q\bar{q}})^2>}{4|<\sigma^N_{q\bar{q}}>|^2} \quad <\dots>=\int d^2\rho\dots|\Psi^L_{\gamma^\star q}|^2 \tag{6.31}$$

The value K depends on the particular choice of the dipole cross-section and should converge to 1.
As the broadening depends on the p_T^{max}, the comparison to experimental data is quite difficult. It would be better to construct a variable from $\delta < p_T^2 >$, which is independent on p_T^{max}. For example

$$< \sigma^{pN} p_T^2 > := \int_0^{p_T^{max}} d^2 p_T p_T^2 \sigma^{pN}(p_T, \alpha) \tag{6.32}$$

diverges logarithmically for $p_T^{max} \to +\infty$. Since a divergence type is the same as for a nuclear case, so the variable

$$\delta < \sigma p_T^2 > := < \sigma^{pA} p_T^2 > - A < \sigma^{pN} p_T^2 > \tag{6.33}$$

is independent of any cut-off, because divergencies cancel themselves. Although it cannot be measured directly, it is far better variable for the comparison with data.

Chapter 7

Results and predictions

Now, results of the computation using a color dipole approach will be presented. First of all, let's discuss the applicability of this model. It has to be pointed out that although both valence and sea quarks are taken into account in distribution functions, in color dipole scheme only the pomeron exchange is included and so the valence content is ignored. It corresponds to a situation when the reggeon part of a dipole cross section is neglected and the sea part(pomeron) dominates. That is particularly convenient in very high energy collisions. The range of validity is not known exactly, but it was suggested[9] that it is meaningful for $x_2 < 0.1$. Our parametrization comes from a fit to the DIS data for $x_{Bj} < 0.01$ and $Q^2 < 500\text{GeV}^2$. Most of data available for the comparison do not fit to this kinematic range and furthermore they are integrated over x_F and M^2 and so there are contributions not involved in the color dipole approach.
For the purpose of comparison, data for the DY process from p-p collisions at the E866 experiment[7] corresponding to the energy 800GeV in a lab. frame will be used. Parameters x_F and M are chosen such that they agree with mean values of the interval

$$0.55 < x_F < 0.8 \quad < x_F >= 0.63 \tag{7.1}$$

$$4.2 < M_{\mu^+\mu^-} < 5.2 \quad < M >= 4.8 \tag{7.2}$$

$$5.2 < M_{\mu^+\mu^-} < 6.2 \quad < M >= 5.7 \tag{7.3}$$

Besides it has to be pointed out that it is necessary to include a non-zero quark mass m_q. The reason is that LC wave functions are dominated by contributions from modified Bessel functions of the second kind K_0 and K_1 that diverge as the argument approaches 0. For the DY process, it is not so important since the argument is enhanced by a dilepton part $\sim M^2$. But for the inclusive direct photon production, where $M^2 = 0$, the argument is determined by a chosen value of a quark mass. The calculation however do not depend overly on a particular value of this mass.

The quantity we will compare to data is an invariant cross-section $E\frac{d^2\sigma}{d^3p}$ which is connected to our derivations as

$$E\frac{d^3\sigma}{d^3p} = \sqrt{M^2 + p_T^2 + x_F^2}\frac{s}{4}\frac{2}{\sqrt{s}}\frac{d^3\sigma}{d^2p_T dx_F} \tag{7.4}$$

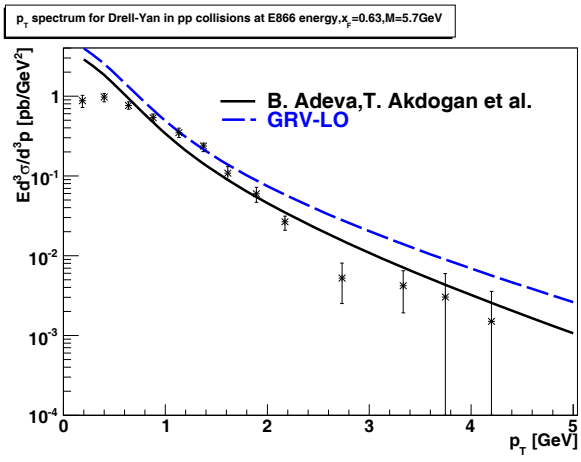

Figure 7.1: The Drell-Yan p_T spectrum from E866 compared to the color dipole approach model using two distribution functions, $x_F = 0.63$, $M = 5.7$GeV

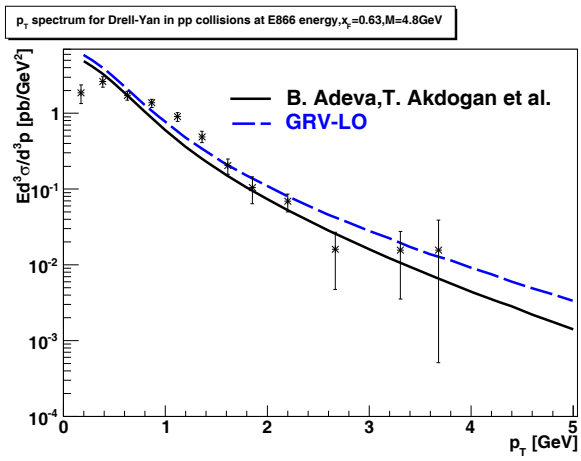

Figure 7.2: The Drell-Yan p_T spectrum from E866 compared to the color dipole approach model using two distribution functions, $x_F = 0.63$, $M = 4.8$GeV

Results suggest that color dipole calculations do not describe a region $p_T \to 0$ very well. But the fact, that in this limit the DY cross-section do not diverge as in LO pQCD shows the advantages of such description. One of the possibilities why data do not match can be a soft non-perturbative primordial p_T distribution of partons in proton. Moreover, experimental data for $p_T \to 0$ should be taken with care since there exist a contradiction amongst several experiments for the DY pair production in low p_T. For example experiments E772 and E866[7] are in a good agreement through the whole p_T spectra of a dilepton except for the region $p_T \to 0$ where they disagree.
Next, the DP production is tested under same conditions. Now, the $x_F = 0$ and $M^2 = 0$, so there is no need to select any average values. Results are compared to data from the experiment PHENIX[8] for p-p collisions at the energy $\sqrt{s} = 200GeV$ in a midrapidity.

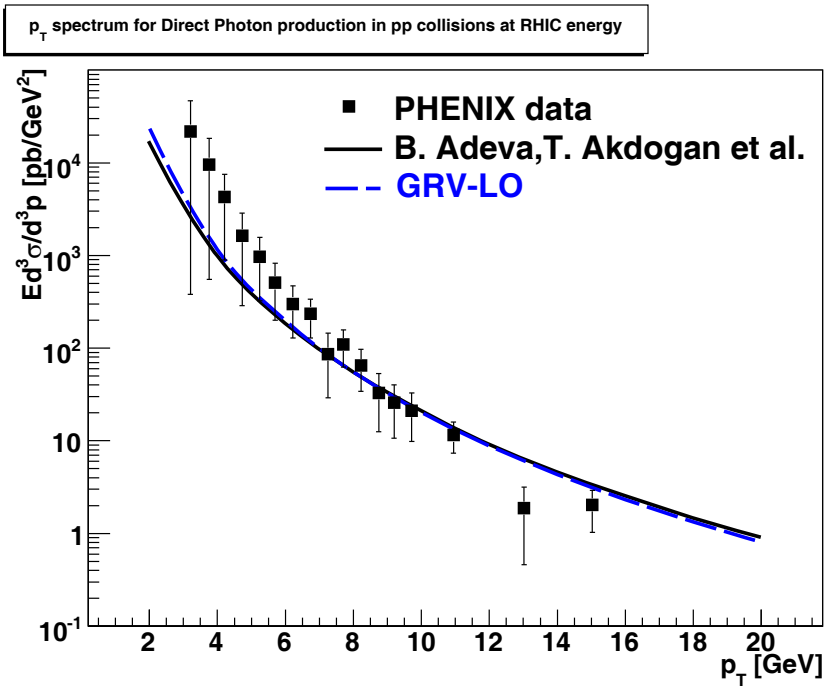

Figure 7.3: The Direct Photon p_T spectrum from PHENIX compared to the color dipole approach model using two distribution functions

Results suggest that this model do not give a good approximation to data. But it has to be stated that both lines lie within experimental errors and so it can be used for further analysis.
Further predictions from this model will be nuclear effects for the Drell-Yan and the Direct Photon production in p-A and d-A collisions. Since there are no data

to compare, they have to serve as a prediction of measurable phenomena. These effects can be described by corresponding nuclear modification factors(see 6.8 6.9). For the DY production in p-A collisions assuming $x_F = 0.6$ and $M = 6$GeV

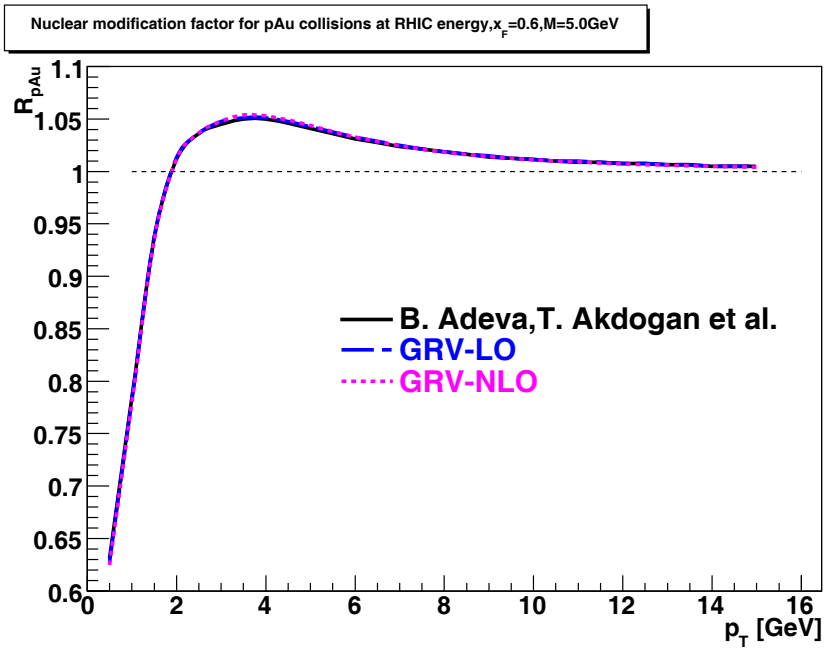

Figure 7.4: The dependence of a nuclear modification factor for the DY process in p-A collisions on three distribution functions

It is obvious that at small p_T there is a strong suppression due to the shadowing. In the central region there is an enhancement of a p-A cross-section known as the Cronin effect, caused by the nuclear broadening. The magnitude of Cronin enhancement is approximately 10%. For large p_T the modification factor converges to 1. It corresponds to an idea that for large p_T valence quarks in a proton distribution function dominates over all other factors and R_{pA} converges to

$$\frac{\int_{x_1}^{1} AF_2^p d\alpha}{A\int_{x_1}^{1} F_2^p d\alpha} = 1 \tag{7.5}$$

Differences between proton distribution functions are nearly negligible. The dependence of this ration on the choice of M and x_F is depicted on following figures.

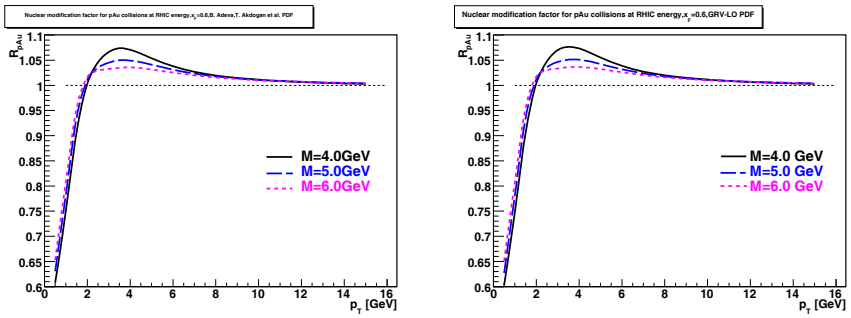

Figure 7.5: The dependence of R_{pA} on the choice of M for both PDF's. On the left, the Adeva-Akdogan parametrization is used. On the right, the GRV-LO parametrization is used

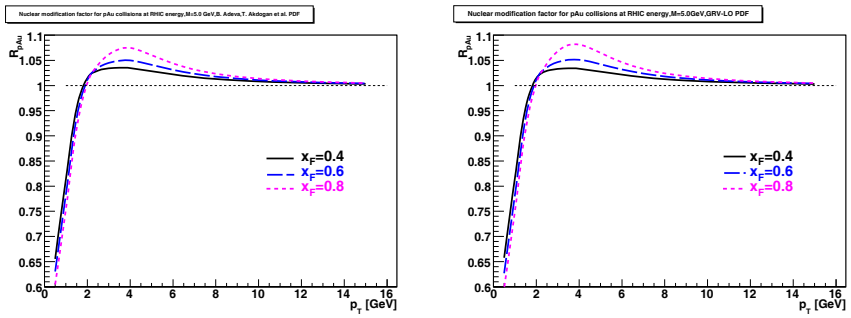

Figure 7.6: The dependence of R_{pA} on the choice of x_F for both PDF's. On the left, the Adeva-Akdogan parametrization is used. On the right, the GRV-LO parametrization is used

It can be seen that the Cronin enhancement decrease with increasing M and decreasing x_F.
For the DP production, results are summarized in the following figure. Since x_F and M are obsolete in DP scheme, they are fixed at zero.

The course is similar to the DY case, but here there starts to be a difference between both parametrizations mainly in the magnitude of a Cronin effect. It differs by 10% approximately. However, this increase is compensated by the level of shadowing, therefore the area under both curves remain the same. That indicates the consistency of this prediction. The convergence for large p_T remain here preserved similar to the DY.

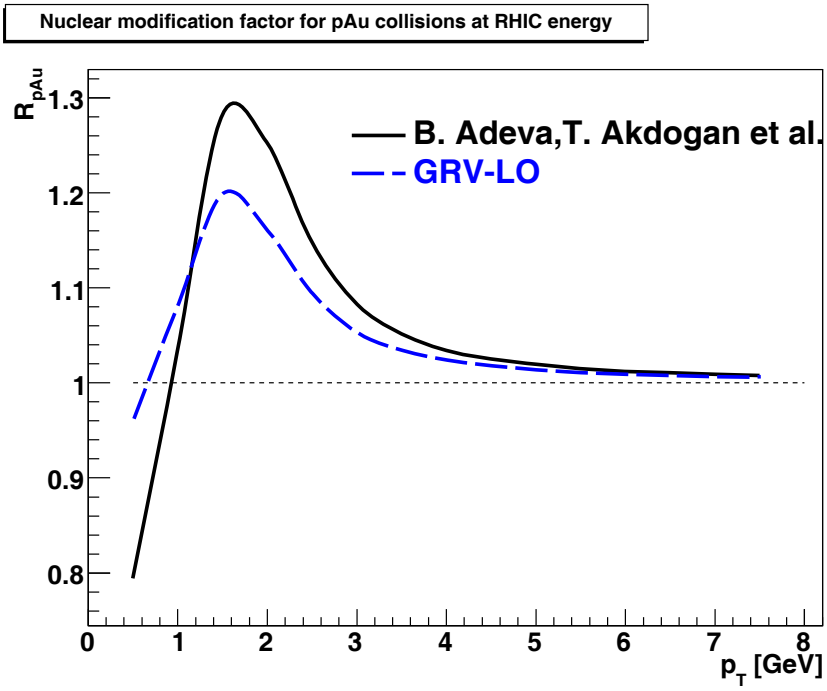

Figure 7.7: The dependence of a nuclear modification factor for the DP process in p-A collisions on two distribution functions

If we pass over to d-A collisions, the DY production predict the course

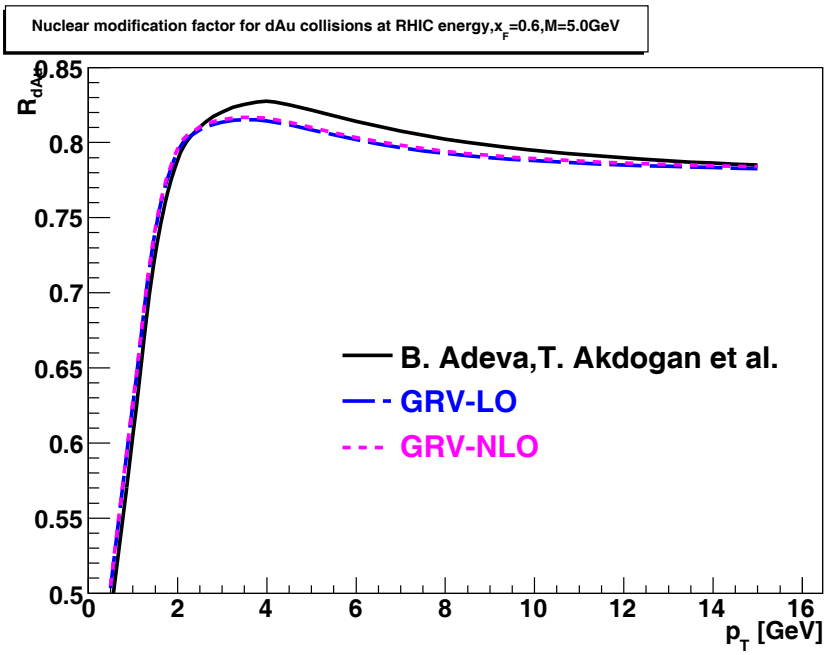

Figure 7.8: The dependence of a nuclear modification factor for the DY process in d-A collisions on three distribution functions

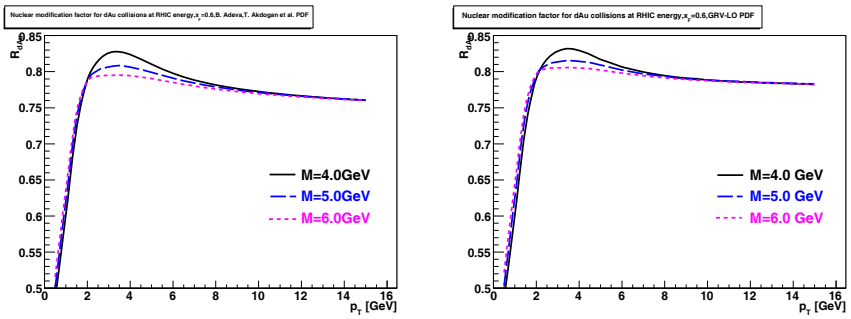

Figure 7.9: The dependence of R_{dA} on the choice of M for both PDF's

In this case, for large p_T curves should converge to the value

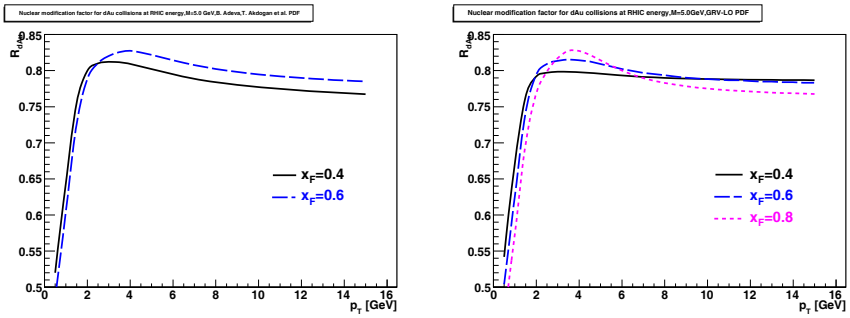

Figure 7.10: The dependence of R_{dA} on the choice of x_F for both PDF's

$$\frac{\int_{x_F}^{1} AF_2^d}{2A\int_{x_F}^{1} F_2^p} \sim 0.77 - 0.83 \tag{7.6}$$

which is in agreement with results. A course and a dependence of other effects agrees with results for the p-A factor. The convergence in the case of x_F dependence vary with different x_F as can be seen from the formula above. In a figure describing the x_F dependence of R_{dA} for the first PDF the value $x_F = 0.8$ cannot be taken into account since this PDF has a validity range up to $x_F = 0.85$ and so the integration ranges are out of the validity range.
Similar for the DP production

where the convergence is given by the formula

$$\frac{\int_{0}^{1} AF_2^d}{2A\int_{0}^{1} F_2^p} \sim 0.83. \tag{7.7}$$

Curves for both parametrizations differ again, but only such that the integral remain constant.

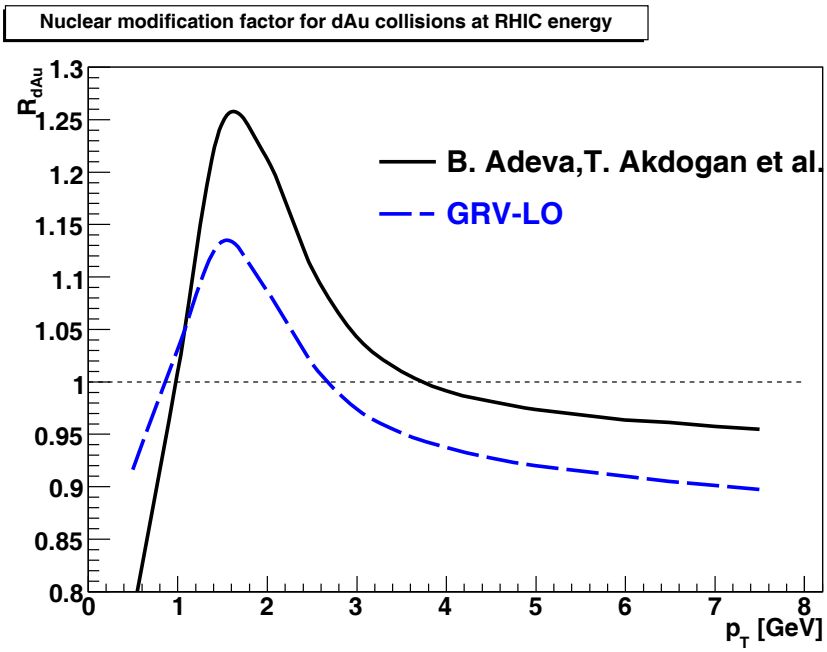

Figure 7.11: The dependence of a nuclear modification factor for the DP process in d-A collisions on two distribution functions

Chapter 8

Summary and Conclusions

The color dipole approach was used to calculate the cross-section and p_T spectrum of the Drell-Yan and the Direct Photon production. The comparison with data shows a good agreement and therefore usefulness of this approach for nuclear predictions. Nuclear modification factors are presented for p-A and d-A collisions for both processes. They reconstruct all expected phenomena - nuclear shadowing, Cronin effect and the convergence. Also the dependence of both factors on x_F and M is presented for the DY process. The magnitude of Cronin effect vary with different x_F and M as was predicted. Results show that

- The DY spectrum is described pretty well for both PDF's for $p_T > 0.5$GeV. For lower p_T data are not easy to describe using our model. Both PDF's then differ considerably at high p_T.
- The DP spectrum do not match very well with data in low p_T region. For $p_T > 7$GeV the description of data is considerably improved. Both PDF's give almost the same predictions that lies within experimental errors.
- The nuclear modification factor for the DY in p-A collisions shows quite strong suppression for $p_T < 2$GeV due to the shadowing. In the region between 2 and 6GeV, the Cronin enhancement of 5% can be seen. For high p_T the convergence to 1 is reconstructed.
- The nuclear modification factor for the DP in p-A collisions shows the shadowing for $p_T < 1$GeV. The Cronin effect is here $20 - 30\%$ according to the PDF used. Difference between both parametrizations seems quite strong but the overall integral of both lines and the high p_T limit are the same for both PDF's which indicate consistency of a prediction.
- The nuclear modification factor for the DY in d-A collisions indicate the same behavior as for p-A. The value of the Cronin enhancement is again about 5%.

- The nuclear modification factor for the DP in d-A collisions differs considerably for each PDF. The Cronin enhancement is approximately 5% lower that in the p-A case. The convergence for the GRV parametrization is faster than for the other PDF, but both converge to the proper value 0.83

These predictions are performed for energies corresponding to the RHIC accelerator. Further progress can be made towards the LHC energies. Furthermore, there are some effects that can be included into the PDF to describe phenomena like the EMC effect. That will be the aim of further analysis

Appendices

The Glauber-Gribov eikonalization theory

For the purpose of the derivation of $\sigma_{q\bar{q}}^{A}$ and therefore nuclear effects also, it is essential to analyze multiple scattering of a hadron fluctuation inside a target. In general, it can be described by the optical model of a Glauber-Gribov theory. Basics of this theory were formulated by Glauber[13] for non-relativistic quantum mechanics. The optical model comes from the eikonal approximation under condition that different scattering phases are additive. That model was generalized by Gribov[14] for the relativistic quantum field theory, but only up to the double scattering. Final scattering amplitude for a nucleus is then given by a sum of all amplitudes from multiple scattering[13]

$$F(s) = \sum_{n=1}^{A} F^{(n)}(s) \tag{1}$$

$$F_S^{(n)} = \left(\frac{i}{k}\right)^{n-1} \int d^2b \int_{\mathbb{R}} dz_1 \rho_A(b, z_1) \int_{z_1}^{+\infty} dz_2 \rho_A(b, z_2) \dots \int_{z_{n-1}}^{+\infty} dz_n \rho_A(b, z_n)$$
$$\sum_h f_{\gamma^\star \to h_1} e^{-iq_L^{\gamma^\star \to h_1}(z_2 - z_1)} f_{h_1 \to h_2} e^{-iq_L^{h_1 \to h_2}(z_3 - z_2)} \dots f_{h_{n-1} \to \gamma^\star}$$

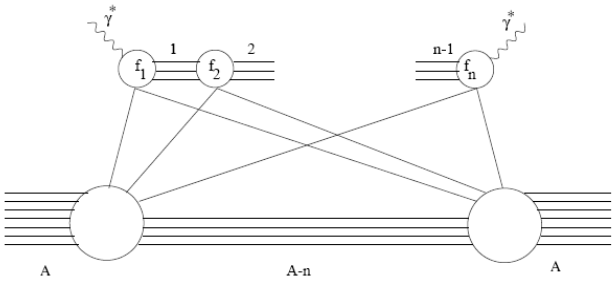

Figure 1: The n-fold scattering amplitude scheme with n-1 intermediate hadronic states

The assumption is that the impact parameter does not change during the collision. Integration ranges take into account that $i+1$th collision can happen after the ith one. After the first collision, the virtual photon pass over to a multiparticle hadronic state h_1. The scattering amplitude of such process is denoted as $f_{\gamma^\star \to h_1}$. Furthermore, the transfer of longitudinal momentum $q_L^{\gamma^\star \to h_1}$ is manifested as oscillating phase factor for all intermediate states

$$q_L^{\gamma^\star \to h_1} = \frac{Q^2 + M_{h_1}^2}{2\nu} \tag{2}$$

In the end, the summation over all possible intermediate states is needed. According to the optical theorem, the final cross-section can be written as

$$\begin{aligned} \sigma_{tot} &= \frac{4\pi}{k} Im(f(0)) \\ &\Downarrow \\ \sigma^{\gamma^\star A}(s) &= \frac{2F(s)}{k} \end{aligned} \tag{3}$$

There is, of course, a problem that these intermediate states are not known. Here comes the idea to interpret a virtual photon as a superposition of hadrons with the same quantum numbers - vector mesons. This is so called generalized vector dominance model (GVDM). Therefore, invariant masses of fluctuations are fixed, but still transition amplitudes between fluctuations are not known. Here, we introduce the vector dominance model(VDM), where all non-diagonal transitions are omitted. It says, that we take only mesons that have a meson-nucleon cross-section $\sigma_{Vp} \sim \frac{1}{M_V^2}$. Such steep decrease of a cross-section leads to the fact that shadowing appears as a higher loop effect and therefore do not vanish at high Q^2(Gribov paradox). The shadowing has to fulfil two conditions

- A mean free path of hadronic fluctuation has to be long enough to experience multiple scattering

$$\frac{1}{\rho_A \sigma_{eff}} << R_A$$

- A coherence length l_c has to be greater than the internucleon separation

In order to determine scattering amplitudes for higher scattering, we will use the knowledge of interaction eigenstates. In this set, there are no non-diagonal transitions. The problem is, that masses of eigenstates are to be determined for a given l_c. But such masses are not defined in a mixed representation and so we cannot evaluate it properly. Only in the limit $l_c \to +\infty$ the whole expansion can be summed in the eikonal form

$$\begin{aligned} \sigma^{\gamma^\star A} &= 2\int d^2b \int_0^1 d\alpha \int d^2\rho |\Psi_{q\bar{q}}(\alpha,\rho)|^2 \left(1 - e^{-\frac{\sigma_{q\bar{q}}(s,\rho)T_A(b)}{2}}\right) + \\ & 2\int d^2b \int_0^1 d\alpha \int \frac{d\alpha_G}{\alpha_G} \int d^2\rho_1 d^2\rho_2 |\Psi_{q\bar{q}G}(\alpha,\alpha_G,\rho_1,\rho_2)|^2 . \\ & \left(1 - e^{-\frac{\sigma_{q\bar{q}G}(s,\rho_1,\rho_2)T_A(b)}{2}}\right) + \ldots \end{aligned} \tag{4}$$

Restricting ourselves to the first order, we can write

$$\sigma^{\gamma^\star A} = \left\{ 2\int d^2b \left(1 - e^{-\frac{\sigma_{q\bar{q}}(s,\rho)T_A(b)}{2}}\right) \right\}, \tag{5}$$

where

$$\{\dots\} = \int_0^1 d\alpha \int d^2\rho |\Psi_{q\bar{q}}(\alpha,\rho)|^2 \dots \tag{6}$$

This is a difference from a glauber eikonal approximation, where

$$\sigma^{\gamma^\star A} = 2\int d^2b \left(1 - e^{-\frac{\sigma_{q\bar{q}}(s,\rho)T_A(b)}{2}}\right) \tag{7}$$

and is called Gribov inelastic correction[14]. But that is valid only where l_c is sufficiently large and ρ can be considered constant, i.e. for very big energies.

Chapter 9

References

[1] B. Z. Kopeliovich, A. H. Rezaeian, H. J. Pirner, Ivan Schmidt, Phys.Lett. B653 (2007) 210-215

[2] B.Z. Kopeliovich, J. Raufeisen, A.V. Tarasov, M.B. Johnson, Phys.Rev. C67 (2003) 014903

[3] J. Raufeisen, QCD coherence effects in high energy reactions with nuclei, PhD-thesis, arXiv:hep-ph/0009358v1, 2000

[4] B. Adeva,T Akdogan et. al., Phys. Rev. D,58,11(2002)

[5] M.Gluck, E.Reya, A.Vogt, Z.Phys. C67:433-448,1995

[6] J.M.Campbell, J.W.Huston and W.J.Stirling, Hard interactions of quarks and gluons: a primer for LHC physics, Rep. Prog. Phys. 70(2007) 89-193

[7] J.C.Webb, Measurement Of Continuum Dimuon Production In 800-GeV/C Proton-Nucleon Collisions, PhD-thesis, arXiv:hep-ex/0301031v1, 2003

[8] PHENIX Collaboration, Phys. Rev. Lett. 98, 012002 (2007)

[9] A.B.Zamolodchikov, B.Z.Kopeliovich and L.I.Lapidus, JETP Lett. 33, 595 (1981)

[10] K.Golec-Biernat and M.Wusthoff, Phys. Rev. D59, 014017 (1999); D60, 114023 (1999)

[11] S.D.Drell and T.Yan, Phys. Rev. Lett. 25, 316 (1970) [Erratum-ibid. 25, 902 (1970)]

[12] C.S.Lam and W.-K.Tung, Phys. Rev. D 18, 2447 (1978); Phys. Rev. D 21, 2712 (1980)

[13] R.J.Glauber "High Energy Collision theory" in Lectures in Theoretical Physics, vol. 1, W.E.Brittin and L.G.Duham (eds.) Interscience, New York, 1959 V. N.

[14] Gribov, Sov. Phys. JETP 30 (1970) 709; [Zh. Eksp. Teor. Fiz. 57 (1969) 1306]

[15] L. D. Landau and I. J. Pomeranchuk, Dokl. Akad. Nauk SSSR 92, (1953) 535, English translation in The Collected Papers of L. D. Landau, sections 75, p. 586 Pergamon Press, (1965)

[16] A. B. Migdal, Phys. Rev. 103, (1956) 1811

9.1 Bibliography

[1] E.Byckling, K.Kajantie, Particle kinematics, John Wiley and Sons New York, USA, 1973

[2] http://www.helsinki.fi/ www_sefo/kinematics/lectures/

[3] S.Donnachie, G.Dosch, P.Landshoff, O.Nachtmann, Pomeron physics and QCD, Cambridge university press, The United Kingdom, 2002

[4] P.D.B.Collins, An introduction to Regge theory and high energy physics, Cambridge university press, The United Kingdom, 1977

[5] M. Abramowitz and I. A. Stegun, Handbook of Mathematical Functions, Dover Publications Inc., New York, USA, 1972

[6] W.H.Press, S.A.Teukolsky, W.T.Vetterling, and B.P.Flannery, Numerical Recipes in Fortran, 2nd edition, Cambridge University Press, New York, 1992